Introduction

The nuclear receptor family is a large group of ligand-dependent or ligand-independent transcription factors with 48 genes identified in the human genome. There is accumulating evidence that nuclear receptors are very fascinating components in terms of biological relevance to human diseases such as cancer, heart diseases, diabetes, and other lifestyle-related diseases or regulatory functions by natural and synthetic ligands. However, because of the multifunctional properties of individual nuclear receptor, the precise molecular behavior of nuclear receptors under physiological circumstances is still far from being completely understood. In addition, nuclear receptors have long been attractive drug targets and provide an enormous body of knowledge about the medicinal chemistry of their small molecule modulators. Importantly, many of the nuclear receptors are druggable targets, which is why numerous natural and synthetic nuclear receptor ligands, mostly composed of the steroid structural class, are on the market. The huge economic impact of those ligands is represented by their estimated share of 10–15% of the global pharmaceutical market. Many nuclear receptors are known as intrinsic components of immune responses including glucocorticoid receptor (GR), retinoic acid receptors (RARs), vitamin D receptor (VDR), peroxisome proliferator-activated receptors (PPARs), and retinoid orphan receptors (RORs). Herein, we discuss our recent findings that orphan nuclear receptor NR4A2 is profoundly involved in the development of autoreactive T cells and to be added to the list of beneficial molecular targets for autoimmune diseases such as multiple sclerosis.

Functions of NR4A2 Orphan Nuclear Receptor

The members of the NR4A subfamily are expressed mostly at low levels in a wide variety of metabolically demanding and energy-dependent tissues such as skeletal muscle, adipose tissue, heart, kidney, liver, and brain [1]. On certain stimuli, however, they are induced to express at very high levels, reminiscent of immediate/early genes. The diversity of signals leading to their expression suggests that they function in a highly cell-type and context-dependent manner. NR4A2 is mainly expressed in the central nervous system (CNS), especially in the cortex, ventral midbrain, brainstem, and spinal cord.

In general, nuclear receptors are composed of several conserved functional domains including DNA-binding domain (DBD) with two zinc fingers in the N-terminal region of the molecule and ligand-binding domain (LBD) in the C-terminal region with less conserved structures. In the absence of specific ligands, most of the nuclear receptors are inactive through interacting with co-repressor protein. Upon ligand binding to a hydrophobic cleft in the LBD, a conformational repositioning occurs at the C-terminal amphipathic α-helix (H12) of the LBD that provide a well-defined surface (activation-function 2, AF-2) recognized by co-activator

Table 1 NR4A2 expressed in autoreactive T cells mediates production of inflammatory cytokines and autoimmune response

Intervention	Target	Readout	IL-17
Transfection of NR4A2 plasmid	EL4	Promoter activity (luciferase assay)	↑
Infection of NR4A2-encoding retrovirus	Murine CD4 T cell	Protein expression	↑
NR4A2-specific siRNA	Murine CD4 T cell	Protein expression	↓
NR4A2-specific siRNA	Human CD4 T cell	Protein expression	↓
NR4A2-specific siRNA	PLP-reactive T cell	Experimental autoimmune encephalomyelitis induction (passive EAE)	↓

proteins, leading to the formation of a multiprotein complex mediating gene activation such as histone acetylation and other chromatin modifications. However, NR4A2 would encode unusual and atypical LBDs that lack canonical ligand-binding properties. Therefore, NR4A2 is believed to be a ligand-independent and constitutively active receptor, and its activity is tightly controlled at the level of gene expression, posttranscriptional modification, and multivalent complex formation with other molecules. The DNA-binding motif for the NR4A family members is the octanucleotide 5′-A/TAAAGGTCA (NGFI-B response element, NBRE) where NR4A2 binds as monomers and homodimers. The pro-opiomelanocortin gene promoter contains another class of transcriptional target of homodimers (Nur-responsive element, NurRE) with an inverted repeat of the NBRE-related octanucleatide, AAAT(G/A)(C/T)CA. NR4A1 and NR4A2 also bind as heterodimers with the retinoid X receptor (RXR) and bind a motif called DR-5. In addition, multivalent complex formation of NR4A2 with other transcription factors enables it to show noncanonical DNA binding.

NR4A2-deficent neonates die at birth because of a severe defect in respiratory function even with having intact NR4A1/3 genes, suggesting the unique functional property of NR4A2. Because of the selective expression of NR4A2 in the CNS, most of the target genes of NR4A2 known to date are limited to this region. For instance, NR4A2 is shown to play a role in the transcriptional activation of tyrosine hydroxylase involved in the synthesis of dopamine. Another group of NR4A2 target genes resides in those relevant to bone formation, such as osteopontin and osteocalcin. NR4A1 (also known as Nur77) and NR4A3 (NOR-1) are suggested to be expressed in thymus and mediate T-cell receptor-mediated T-cell apoptosis; however, distribution and function of NR4A2 in immune cells is not well elucidated. Meanwhile, there is accumulating evidence suggesting the pivotal roles of NR4A family members on inflammatory responses and that they are aberrantly expressed in inflamed synovial tissue of rheumatoid arthritis, psoriatic skin, and atherosclerotic lesions. Therefore, NR4A receptors may contribute to the cellular processes that control inflammatory disorders including autoimmunity (Fig. 1).
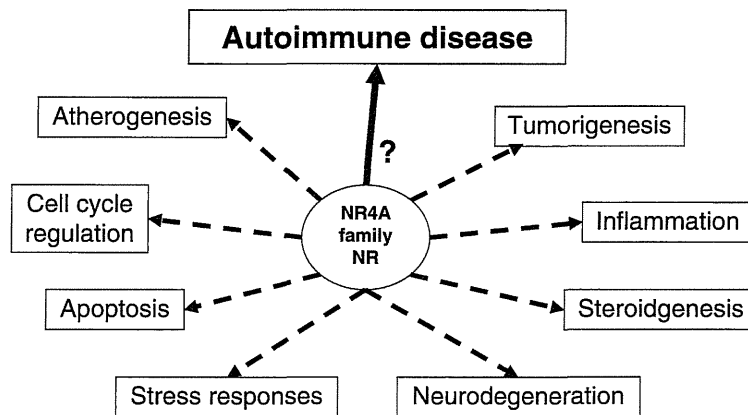
Fig. 1 Versatile function of NR4A2 on various biological responses. *NR* nuclear receptor

NR4A2 in Autoimmunity

Multiple sclerosis (MS) is a chronic inflammatory disease of the CNS, accompanying multiple foci of inflammatory demyelinating lesions. MS is thought to have an autoimmune pathogenesis, which is mediated by autoimmune T cells reactive to myelin antigens such as myelin basic protein (MBP), myelin oligodendrocyte glycoprotein (MOG), and proteolipid protein (PLP). Development of inflammatory processes within the CNS is triggered by proinflammatory cytokines and chemokines produced by the autoimmune T cells after their entry into the CNS. Notably, the encephalitogenic T cells need to be preactivated in the periphery before they penetrate into the CNS parenchyma. A large portion of the pathogenic Th cells that mediate autoimmunity secrete proinflammatory cytokines and chemokines after recognizing self-antigen in a major histocompatibility complex (MHC) class II-restricted manner. Previously it was thought that CD4$^+$ IFN-γ-secreting Th1 cells played a central role in causing autoimmune diseases, but the discovery of Th17 cells with a significant pathogenic activity in autoimmunity has opened the gate for new directions of research [2, 3]. Although interleukin (IL)-12 controls Th1 differentiation from naive CD4$^+$ T cells, transforming growth factor (TGF)-β in combination with IL-6 is appreciated as the classical Th17 cell-differentiating cytokine milieu. Th1 cells express the lineage marker transcription factor T-bet; Th17 cells express another transcription factor, ROR-γt. There is now a consensus that both Th1 and Th17 cells contribute to the development of autoimmune disease, including MS, and that the relative contributions of either of these different helper T-cell populations might explain diversity in clinical and pathological manifestations of autoimmune diseases as well as in their response to therapy.

Experimental autoimmune encephalomyelitis (EAE) is a prototype autoimmune disease model that has greatly contributed to elucidating the pathogenesis of MS. EAE can be induced in laboratory animals by active immunization with myelin antigens or by passive transfer of myelin antigen-specific T cells. Because Th1 cell clones reactive to MBP, PLP, or MOG are capable of inducing clinical and pathological

manifestations of EAE in naive mice, Th1 cells producing interferon (IFN)-γ have long been believed to play a central role in the pathogenesis of MS. However, the "Th1 disease" dogma has been challenged by contradicting results obtained from rodent models of MS. Namely, despite obvious lack of Th1 cells, gene-targeted mice deficient for IFN-γ or IFN-γ receptor are still susceptible to EAE. Furthermore, mice deficient for IL-12 signaling were found to develop EAE. Subsequent studies have clarified that IL-23 rather than IL-12 is essential for the development of EAE. Lately, it was revealed that the IL-23-dependent pathogenic T cells would represent Th17 cells, a novel helper T-cell subset characterized by production of IL-17. Currently, it is widely appreciated that Th17 cells play an important role in the development of inflammatory autoimmune diseases, either independently or collaboratively with Th1 cells.

DNA microarray analysis previously revealed upregulation of IL-17 as well as the downstream transcripts in the brain lesions of MS. More recently, a pathological study has demonstrated that IL-17-secreting T cells are present in active rather than chronic lesions of MS. These results indicate that Th17 cells actively participate in the autoimmune inflammation in the MS brain. Gene expression profiling for brain lesions of MS provided a number of potential candidate molecules that might be appropriate as a therapeutic target. Similarly, microarray analysis of peripheral blood could help characterize a disease signature of MS, leading to an identification of potential therapeutic targets. We have previously characterized gene expression profile of peripheral blood T cells derived from Japanese MS patients and found that expression of the nuclear orphan receptor NR4A2 is most significantly augmented in MS compared with healthy subjects [4]. Quantitative reverse transcriptase-polymerase chain reaction (RT-PCR) analysis consolidated the overexpression of NR4A2 in the peripheral T cells of MS, and expression of NR4A2 in T cells from MS showed an approximately fivefold increase compared to those from healthy donors. NR4A2 mutations are well known to cause familial Parkinson's disease, reflecting its essential role in the development and survival of substantia nigra neurons. In contrast, much less attention has been paid to its functional role in T cells. More than a decade ago, NR4A1 and NR4A3 were shown to mediate apoptotic processes of mature as well as immature T cells. However, these studies do not give insights into the functional implication of upregulated expression of NR4A2 in T cells from MS. Therefore, we have begun functional analysis of NR4A2 as an important molecule regulating the Th1/Th17 cell function through expression of key cytokines including IL-17 and IFN-γ in the pathogenesis of MS. Although NR4A2 is a transcription factor of the steroid/thyroid receptor family and has been implicated in various cellular responses such as steroidogenesis, neuronal development, atherogenesis, and cell-cycle regulation, the physiological role of NR4A2 in the development or regulation of T-cell-mediated autoimmune diseases is unknown. Therefore, we have explored the functional involvement of NR4A2 in EAE, a representative rodent model of MS. To explore the possible involvement of NR4A2 in EAE induced in B6 mice by immunization with MOG peptide, T-cell expression of NR4A2 was measured by quantitative RT-PCR. NR4A2 expression in peripheral T cells gave a maximum value on day 21, and the entire expression pattern of NR4A2 in peripheral blood mononuclear cell (PBMC) T cells was well correlated with the clinical severity of EAE. Meanwhile, remarkable expression of NR4A2 was

observed in the CNS-infiltrating T cells on day 9, when an early sign of EAE becomes evident. NR4A2 expression was induced in EAE T cells, but the kinetics of expression significantly differs between PBMC T cells and CNS-infiltrating T cells. Recent studies have indicated that autoimmune Th17 rather than Th1 cells would play a central role in causing autoimmune inflammation, and a major proportion of the CNS-infiltrating cells were found to produce IL-17 or IFN-γ. Therefore, T cells accumulating in the CNS are characterized by massive production of inflammatory cytokines with an intensive expression of NR4A2. The concomitant expression of inflammatory cytokines and NR4A2 in the CNS-infiltrating T cells has guided us to investigate whether NR4A2 directly affects gene expression of inflammatory cytokines as a transcription factor in T cells. Luciferase assay for IL-17 promoter has revealed that transduction of NR4A2 gene would result in upregulation of promoter activity for IL-17 in the EL4 cell line. In addition, NR4A2 transduction by retroviral infection containing NR4A2 gene fragment with GFP into CD4 T cells showed an enhancement of IL-17 expression. Intriguingly, when the small interfering RNA (siRNA) specific for NR4A2 was introduced into encephalitogenic T cells induced after immunization with PLP peptide into SJL mice, progression of clinical disease and histological severity of EAE passively induced by the encephalitogenic T cells was significantly prevented in the siRNA-treated group as compared with control RNA-treated group. Furthermore, evaluation of cytokines in the supernatant has revealed that the siRNA treatment significantly reduced the production of IL-17 by T cells from both healthy donors and MS patients. These results support the important role of NR4A2 in the regulation of cytokine production in pathogenic T cells and modulation of NR4A2 expression by specific siRNAs or putative chemical compounds might be a promising treatment for intervention of active MS that are harboring more potent IL-17-producing T cells [5] (Table 1).

Direct and Indirect Modulators of NR4A2

As summarized in the previous section, we have identified NR4A2 as the most highly upregulated gene among circulating T cells in MS patients. In addition, we observed increased expression of NR4A2 transcripts in the blood and CNS of mice following EAE induction. Forced expression of NR4A2 led to enhanced Th1 and Th17 responses whereas reducing NR4A2 expression decreased the encephalitogenicity of autoimmune T cells in a model of passive EAE. Therefore, NR4A2 has been implicated as a promising molecular target for MS therapy. Intriguingly, the NR4A subfamily of nuclear receptors has been implicated not only in MS but also in rheumatoid arthritis, psoriasis, atherogenesis, Parkinson's disease, schizophrenia, manic depression, Alzheimer's disease, and cancer, which has led to great interest in the identification of selective low molecular weight modulators that is helpful for analyzing the mode of action of the NR4A subfamily [6].

An antineoplastic and antiinflammatory drug, 6-mercaptopurine, has been shown to activate NR4A2, possibly by modulating the cellular content of purine nucleotides. NR4A2 expression is induced by forskolin through the activation of Erk1/2. A number of typical and atypical antipsychotic drugs such as haloperidol, chlorpromazine,

and clozapine induce the transcription of NR4A2. In contrast, methotrexate significantly suppresses expression of NR4A2 in patients with active psoriatic arthritis. Interestingly, the expression level of NR4A2 after treatment with methotrexate is well correlated with disease activity score. In addition, glucocorticoid has been shown to inhibit NR4A2 expression. Although growing numbers of modulators have been described, all these indirect modulators are selective enough to intervene NR4A2 activity. Therefore, the therapeutic utility of NR4A2 will depend on whether novel modulators directly interacting with NR4A2 can be developed.

Using a NR4A2 luciferase reporter gene assay, a number of micromolar activators of NR4A2 has been identified in a combinatorial library of benzimidazole, which has a structural overlap with known nuclear receptor ligands [7]. After screening of substituents having a structurally different moiety, a couple of potent NR4A2 activators ($EC_{50} = 8$–70 nM) was developed based on this benzimidazole scaffold. Another approach using a similar reporter gene assay identified a novel class of NR4A2 activators, isoxazolo[4,5-c]pyridin-4-one [8]. After screening of substituents having a structurally different moiety, a couple of very potent NR4A2 activators ($EC_{50} = 0.8$–3.9 nM) were developed based on this scaffold. Through pharmacokinetic experiments, some of these compounds have been shown to have excellent oral bioavailability and rapid distribution in mice. Even though most of these compounds are NR4A2 agonists, there is another class of NR4A2 modulators, 1,1-bis(3'-indolyl)-1-(p-substituted phenyl) methanes, that provide both NR4A2 agonist and antagonist [9] (Fig. 2). Ligands for RXR are
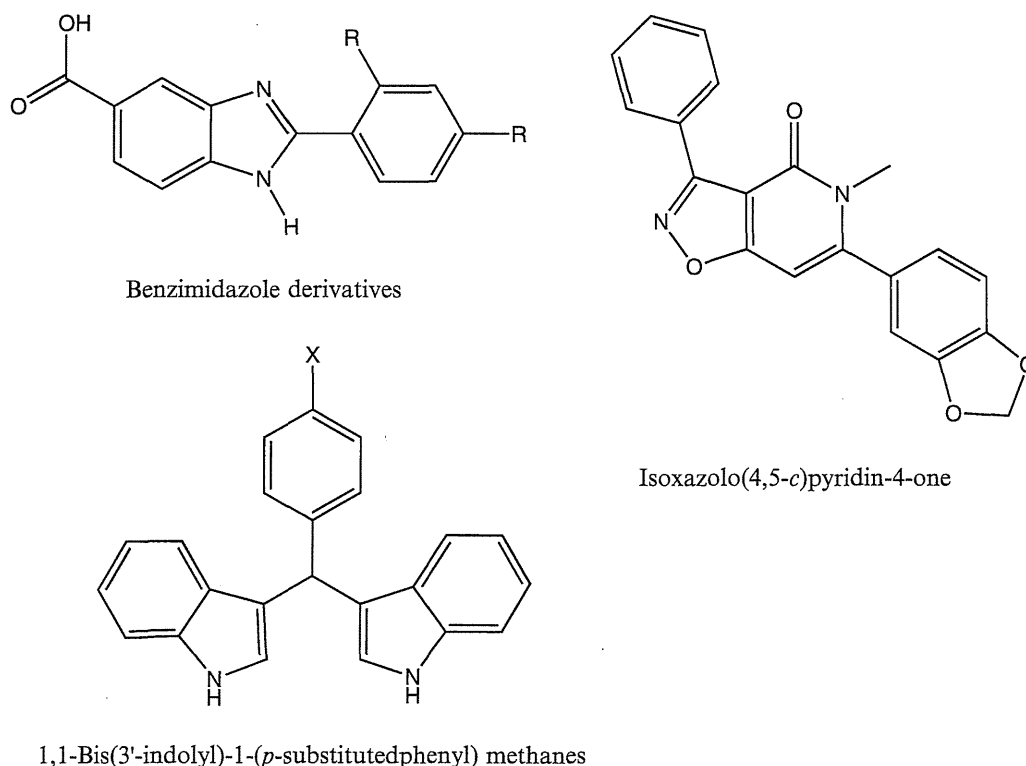

Benzimidazole derivatives

Isoxazolo(4,5-c)pyridin-4-one

1,1-Bis(3'-indolyl)-1-(p-substitutedphenyl) methanes

Fig. 2 Known chemical structures directly modulating NR4A2 function. R represents alkyl side chain; X is either H, OH, OMe, or CF3

another class of potent NR4A2 modulators as RXR potentially forms a heterodimer with NR4A2. The weak RXR agonist HX600 was found to activate NR4A2-RXR heterodimers [10].

Conclusion

We have demonstrated that NR4A2 may represent a promising target for MS and other autoimmune diseases. There were some clinical trials for MS of neutralizing the relevant cytokines IL-17 and IL-23 by specific antibodies, neither of which revealed significant beneficial effects on MS symptoms. Our results demonstrated that NR4A2 acts as an early event in the differentiation of pathogenic T cells, and thus modulating NR4A2 activity may allow a more complete inhibition of effector responses of pathogenic T cells compared with cytokine neutralization.

References

1. Maxwell MA, Muscat GE (2006) The NR4A subgroup: immediate early response genes with pleiotropic physiological roles. Nucl Recept Signal 4:e002
2. Aranami T, Yamamura T (2008) Th17 cells and autoimmune encephalomyelitis (EAE/MS). Allergol Int 57(2):115–120
3. McFarland HF, Martin R (2007) Multiple sclerosis: a complicated picture of autoimmunity. Nat Immunol 8(9):913–919
4. Satoh J, Nakanishi M, Koike F, Miyake S, Yamamoto T, Kawai M et al (2005) Microarray analysis identifies an aberrant expression of apoptosis and DNA damage-regulatory genes in multiple sclerosis. Neurobiol Dis 18(3):537–550
5. Doi Y, Oki S, Ozawa T, Hohjoh H, Miyake S, Yamamura T (2008) Orphan nuclear receptor NR4A2 expressed in T cells from multiple sclerosis mediates production of inflammatory cytokines. Proc Natl Acad Sci USA 105(24):8381–8386
6. Mattes H (2008) NR4A Subfamily of receptors and thier modulators. In: Ottow E, Weinmann H (eds) Nuclear receptors as drug target. Methods and principles in medicinal chemistry, vol 39. Wiley-VCH, New York
7. Dubois C, Hengerer B, Mattes H (2006) Identification of a potent agonist of the orphan nuclear receptor Nurr1. ChemMedChem 1(9):955–958
8. Hintermann S, Chiesi M, von Krosigk U, Mathe D, Felber R, Hengerer B (2007) Identification of a series of highly potent activators of the Nurr1 signaling pathway. Bioorg Med Chem Lett 17(1):193–196
9. Chintharlapalli S, Burghardt R, Papineni S, Ramaiah S, Yoon K, Safe S (2005) Activation of Nur77 by selected 1,1-bis(3'-indolyl)-1-(p-substituted phenyl) methanes induces apoptosis through nuclear pathways. J Biol Chem 280(26):24903–24904
10. Morita K, Kawana K, Sodeyama M, Shimomura I, Kagechika H, Makishima M (2005) Selective allosteric ligand activation of the retinoid X receptor heterodimers of NGFI-B and Nurr1. Biochem Pharmacol 71(1–2):98–107
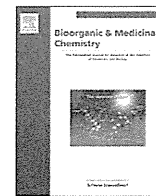
Synthesis and biological evaluation of truncated α-galactosylceramide derivatives focusing on cytokine induction profile

Tetsuya Toba [a], Kenji Murata [a], Junko Futamura [a], Kyoko Nakanishi [a], Bitoku Takahashi [a], Naohiro Takemoto [a], Minako Tomino [a], Takashi Nakatsuka [a], Seiichi Imajo [a], Megumi Goto [a], Takashi Yamamura [b], Sachiko Miyake [b], Hirokazu Annoura [a,*]

[a] Asubio Pharma Co., Ltd, 6-4-3, Minatojima-Minamimachi, Chuo-ku, Kobe 650-0047, Japan
[b] National Institute of Neuroscience, National Center of Neurology and Psychiatry, 4-1-1 Ogawa-Higashi, Kodaira, Tokyo 187-8502, Japan

ABSTRACT

A series of truncated analogs of α-galactosylceramide with altered ceramide moiety was prepared, and evaluated for Th2-biased response in the context of IL-4/IFN-γ ratio. Phytosphingosine-modified analogs including cyclic, aromatic and ethereal compounds as well as the C-glycoside analog of OCH (2) with their cytokine inducing profile are disclosed.

© 2012 Elsevier Ltd. All rights reserved.

1. Introduction

Natural killer T (NKT) cells are potent producers of immunoregulatory cytokines, and are restricted to glycolipid antigens presented by CD1d, a glycoprotein structurally and functionally related to non-classical major histocompatibility complex (MHC) class I.[1] Several natural glycolipids of bacterial[2] and mammalian[3] origin, and quite a few synthetic ligands of CD1d are identified and reported to date.[1b,4] Among them, synthetic α-galactosylceramide KRN7000 (1)[5] (Fig. 1) is the most extensively studied, for its strong activation of NKT cells as well as its effectiveness in in vivo animal disease models.[6] Compound 1 is known to induce various cytokines including proinflammatory Th1 cytokine interferon-γ (IFN-γ) and immunomodulatory Th2 cytokine interleukin-4 (IL-4), which oppose each other's response and may in part result in its marginal effect. Some studies are reported which aim to increase the selectivity of Th1 or Th2 cytokine induction. The majority are directed towards increased Th1 activity, and not few utilize the derivatives of the acyl chain and/or the sugar moiety which are relatively easy to prepare from a synthetic point of view. One of the most potent compounds reported to date is that with 8-(4-fluorophenyl)octanoyl chain as the acyl tail, which binds two orders of magnitude stronger with CD1d than 1.[7] Another impressing finding was the conversion of 1 to its C-glycoside analog 3, which leads
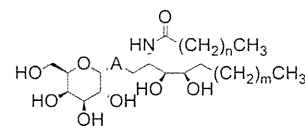
1 (KRN7000; A = O, m = 12, n = 24)
2 (OCH; A = O, m = 3, n = 22)
3 (A = CH₂, m = 12, n = 24)
4 (A = CH₂, m = 3, n = 22)

Figure 1. Structures of KRN7000 (1), OCH (2) and their C-glycoside analogs 3, 4.

to striking enhancement of activity in in vivo animal models of malaria and lung cancer.[8]

An altered analog of 1 termed OCH (2) possessing a shorter phytosphingosine side chain[9] has been identified as NKT cell ligand which predominantly induces IL-4 over IFN-γ. Only compound 2 but not 1 is significantly effective in animal models of Th1-mediated autoimmune diseases such as experimental autoimmune encephalomyelitis (EAE) and collagen induced arthritis (CIA), which makes it an attractive lead for potential therapeutic application.[9,10]

Complete occupation of the binding groove of CD1d by 1 contributes to the sustained stimulation of NKT cells to induce robust immunological response, as indicated by several examples of X-ray crystallographic structures of compound 1/CD1d complex.[11,12] Altered analogs such as 2 with short phytosphingosine chain is considered to result in short duration of stimulation and

* Corresponding author. Tel.: +81 78 306 5047; fax: +81 78 306 5971.
  E-mail address: annoura.hirokazu.wk@asubio.co.jp (H. Annoura).

cause differential polarization of NKT cells.[9d] Instability of the short-chain analogs to form binary and ternary complexes is shown by molecular dynamics simulation study[13] and more directly by using the surface plasmon resonance (SPR) technique.[14] It was also shown that truncation in the phytosphingosine and not the acyl chain will affect the NKT cell activation profile.[14]

As part of our efforts to obtain more potent compounds for the enhancement of Th2 response, a series of analogs based on **2** with altered ceramide moiety was prepared and evaluated in vitro, some of which are the first to be reported. In this report, the structure–activity relationship in the context of IL-4/IFN-γ ratio is described. In the course of our study, the C-glycoside of **2** was prepared for the first time and its cytokine-inducing profile in vitro and in vivo are also described.
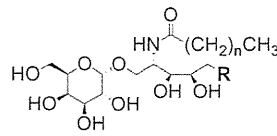
2. Results and discussion

2.1. Chemistry

The analogs were prepared by the versatile method developed by our group (Scheme 1).[15] The phytosphingosine side chain substituents R shown in Tables 1 and 2 were introduced to the known epoxide **5** by means of nucleophilic addition. In addition to the nucleophiles reported earlier utilizing alkyl or aryl lithium reagents or corresponding magnesium bromides,[16] alkoxides and phenoxide were also efficiently introduced. Liquid alcohols were reacted as a solvent, while dioxane was used as a solvent for solid hydroxyls such as phenol. Various nucleophiles, including short or long primary alkyl, secondary alkyl, aryl, alkoxy and aryloxy groups were successfully incorporated via this route. After regioselective mesylation of the more reactive axial hydroxyl group,[17] compound **6** was subjected to benzylidene cleavage and azidation, after which secondary hydroxyl groups were protected to provide isopropylidene acetal **7**. The order of de-benzylidene reaction and azidation could be reversed, but azidation first of the axial mesyloxy group of **6** needed higher temperature, longer time and gave lower yield presumably for its steric demand. On the other hand, azidation later to the deprotected **6** yielded small portions of regio- and stereoisomers as side products along with major product **7**, assumed to have formed via epoxide through nucleophilic addition of the vicinal hydroxyl groups. Generally, deprotection first of **6** gave higher yield in total. Glycosidation with tetra-O-benzyl-α-D-galactosyl fluoride in the presence of BF₃·OEt₂, or with tetra-O-benzyl-α-D-galactosyl bromide or chloride in the presence of tetra-n-butylammonium bromide gave selectively the α-glycoside **9**. The selectivity over the β-isomer was improved in the latter protocol, to a ratio typically greater than 10:1.[15,18] The azido group in **9** was reduced to an amine and acylated with suitable carboxylic

Table 1
Dependency of cytokine induction on alkyl chain lengths[a]

Compound	R	n	IL-4[b] (%)	IFN-γ[b] (%)
11a	–CH₂CH₃	22	105	96
11b	–(CH₂)₂CH₃	21	97	148
11c	–(CH₂)₂CH₃	22	115	112
11d	–(CH₂)₃CH₃	18	6	9
11e	–(CH₂)₃CH₃	20	51	46
11f	–(CH₂)₃CH₃	21	103	93
2	–(CH₂)₃CH₃	22	100	100
11g	–(CH₂)₃CH₃	23	154	103
11h	–(CH₂)₃CH₃	24	129	504
11i	–(CH₂)₃CH₃	26	178	761
11j	–(CH₂)₄CH₃	21	97	113
1	–(CH₂)₁₂CH₃	24	128	569

[a] At 100 ng/ml.
[b] Normalized to **2** at 100 ng/ml.

acids to give **10**. Finally, all the protective groups were removed to give the desired analogs.

It is worthy of note that alkoxy derivatives (e.g., R = n-PrO) or aryl derivatives (e.g., R = Ph) with R at this position are not directly accessible via the Wittig reaction of stereo-fixed, sugar-based starting materials (e.g., D-lyxose).[5a,19]

C-Glycoside **4** was synthesized by short and efficient route as depicted in Scheme 2.[20] Known α-ethynylgalactose derivative **12**[21] and octanal derivative **13** synthesized from L-arabinose were coupled in a chelation-controlled manner to give a 1.6:1 mixture of **14a** and **14b**. Compounds **14a** and **14b** were easily separated by column chromatography over silica gel, and the stereochemistry of the newly formed diastereomeric center was determined for the major isomer **14a** applying modified Mosher's protocol[22] to have the R-configuration.[20] The acetylenic bond in **14a** was selectively and efficiently reduced by diimide reduction, after which the hydroxyl group was mesylated to give **15**. The synthesis of **4** was completed in a straightforward manner, after substitution by azido group, reduction, acylation and global deprotection.
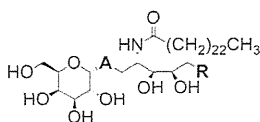
2.2. Biological evaluation

The analogs were evaluated in vitro for their ability to induce IL-4 and IFN-γ relative to **2**. IL-4 and IFN-γ secretion were assessed with spleen cells prepared from C57BL/6 mice, which were
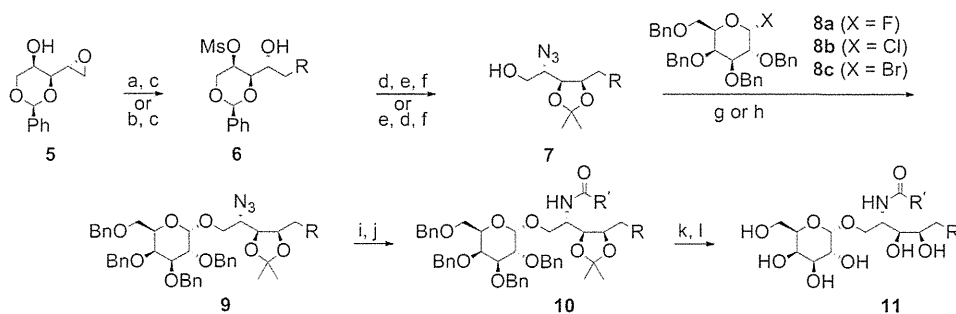
Scheme 1. Synthesis of O-glycosides. Reagents and conditions: (a) RLi or RMgBr, CuI or CuOTf, THF, −40 °C, 52–98%; (b) alcohol or phenol, NaH, (dioxane), rt–80 °C, 83–88%; (c) MsCl, pyridine, −40 °C–rt, 34–93%; (d) H₂, Pd(OH)₂/C, EtOH, rt, or 6 N HCl, MeOH, rt, 68–100%; (e) NaN₃, DMF, 95–110 °C, 20–66%; (f) cat. p-TsOH, 2,2-dimethoxypropane, rt, 26–75%; (g) **8a**, BF₃·OEt₂, MS 4 Å, CHCl₃, −50 °C, 13–73%; (h) **8b** or **8c**, n-Bu₄NBr, MS 4 Å, DMF–toluene, rt, 22–68%; (i) H₂, Lindlar catalyst, EtOH, rt; (j) R'CO₂H, EDCI·HCl, HOBt or HOAt, i-Pr₂NEt, DMF–CH₂Cl₂, 40 °C, 22–100% (two steps); (k) HCl–dioxane, MeOH–CH₂Cl₂, rt, or 80% AcOH, 80 °C; (l) H₂, Pd(OH)₂/C, MeOH–CHCl₃, rt–40 °C, 41–91% (two steps).

Table 2
Cytokine induction profile of the phytosphingosine-altered derivatives and the C-glycoside of OCH[a]

Compound	A	R	IL-4[b] (%)	IFN-γ[b] (%)
2	O	–(CH₂)₃CH₃	100	100
11k	O	–c-Pent	98	74
11l	O	–Ph	211	284
11m	O	–CH₂Ph	57	35
11n	O	–p-Tol	78	76
11o	O	–OCH₃	86	64
11p	O	–O(CH₂)₂CH₃	103	161
11q	O	–O(CH₂)₁₁CH₃	78	227
11r	O	–OPh	99	80
4	CH₂	–(CH₂)₃CH₃	1	0

[a] At 100 ng/ml.
[b] Normalized to **2** at 100 ng/ml.

Figure 2. Side view of the optimized structure of **2** (blue)/hCD1d complex. X-ray structure of **1** (red) is superimposed.

incubated with 100 ng/ml of glycolipids for 72 h. The cytokines in the culture supernatant were measured by ELISA.

Influence of the chain lengths was first examined (Table 1). When the phytosphingosine chain was fixed to that of **2** and acyl chain length altered (compounds **2** and **11d–11i**), the chain length proximal to **2** showed similar cytokine production. As the acyl chain became longer the cytokine release increased, and for chains longer than hexacosanoic acid there was a marked increase in IFN-γ production that dominated IL-4 (**11h, 11i**), which was comparable to **1**. On the other hand, as the chain became shorter the induction of both cytokines decreased rather drastically, and icosanoyl derivative **11d** showed negligible efficacy.

When the acyl chain length was next fixed to that of **2** and sphingosine base altered, in our hands cytokine producing profile did not change for given derivatives (**11a, 11c** and **2**; n = 22). Compounds **11b, 11f** and **11j** which have tricosanoyl chain (n = 21) also showed similar profile. Taking above results together, we concluded that very close modification of **2** both in acyl and sphingosine chain are tolerated and shows similar profiles, and that further shortening of the acyl chain in aim for more Th2-biased response seems inappropriate.

Our interest was next focused on the phytosphingosine moiety, where it makes **2** a completely different switch of the NKT cell signal. Analogs bearing aliphatic ring (**11k**) or aromatic ring (**11l–11n**) were also prepared. To our knowledge, these are the first examples of non-linear hydrocarbon chain analogs of the phytosphingosine moiety that show similar cytokine inducing ratio to **2**.[23] Compound **11l** with an aromatic ring appears to show slight
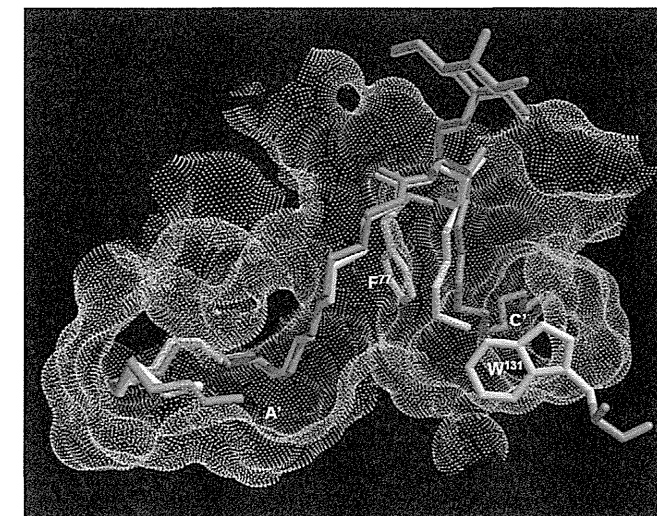
increase in both cytokines. This is suggestive of aromatic interaction(s) with residues such as Phe77 and Trp131 in CD1d (Fig. 2). Aromatic derivatives with one methylene unit longer (**11m**) or one additional methyl in the para-position (**11n**) showed reduced activity, which is indicative of the appropriate length and flexibility in reference to pocket depth, as well as for possible interaction with aromatic residues. We have next prepared analogs bearing ether linkage in the phytosphingosine chain. There is only one report for α-galactosylceramide derivatives with aliphatic ether chain, which assessed the release of IL-2, a Th1 cytokine.[24] Our compounds (**11o–11r**) including oxa- analog of **2** showed similar profiles to corresponding methylene derivatives, which is in line with one example of oxa- analog of **1** shown in the previous report.[24] The oxa- analogs were also shown for the first time to be comparable in the context of IL-4/IFN-γ ratio to the corresponding methylene analogs.

The binding groove of the CD1d consists of two hydrophobic channels A′ and C′ that accommodate two lipid chains of α-glycosyl ceramides. As can be seen from the X-ray structure of **1**/hCD1d complex,[12] the acyl chain occupies A′ pocket and the bent phytosphingosine chain enters the narrow C′ pocket beyond the length of **2** (Fig. 2). We assume the phytosphingosine-altered analogs in Tables 1 and 2 which in length do not reach the C′ pocket showed similar profiles to **2** owing to weak interaction with CD1d. There is a wide space before entering the C′ pocket which allows cycloalkyl and aromatic substituents, and as mentioned earlier the aromatic side chain might interact with aromatic residues such as Phe77 and Trp131. Molecular modeling of **2**/hCD1d complex based on
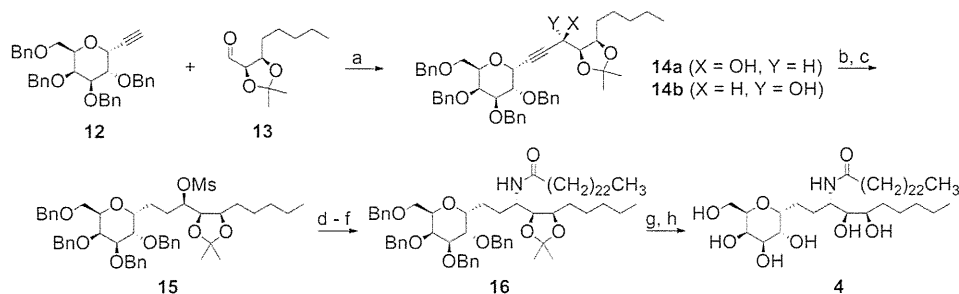
Scheme 2. Synthesis of C-glycoside **4**. Reagents and conditions: (a) n-BuLi, THF, −48 to −30 °C, 47% for **14a**, 30% for **14b** (BRSM); (b) TsNHNH₂, DME, NaOAc aq, reflux, 91%; (c) MsCl, pyridine, CH₂Cl₂, 0 °C–rt, 94%; (d) NaN₃, DMF, 90 °C; (e) H₂, Lindlar catalyst, EtOH, rt; (f) Lignoceric acid, EDCI·HCl, HOAt, Et₃N, DMF–CH₂Cl₂, rt, 48% (three steps); (g) 80% AcOH, 60 °C, 88%; (h) H₂, Pd(OH)₂/C, MeOH–CH₂Cl₂, rt, quant.
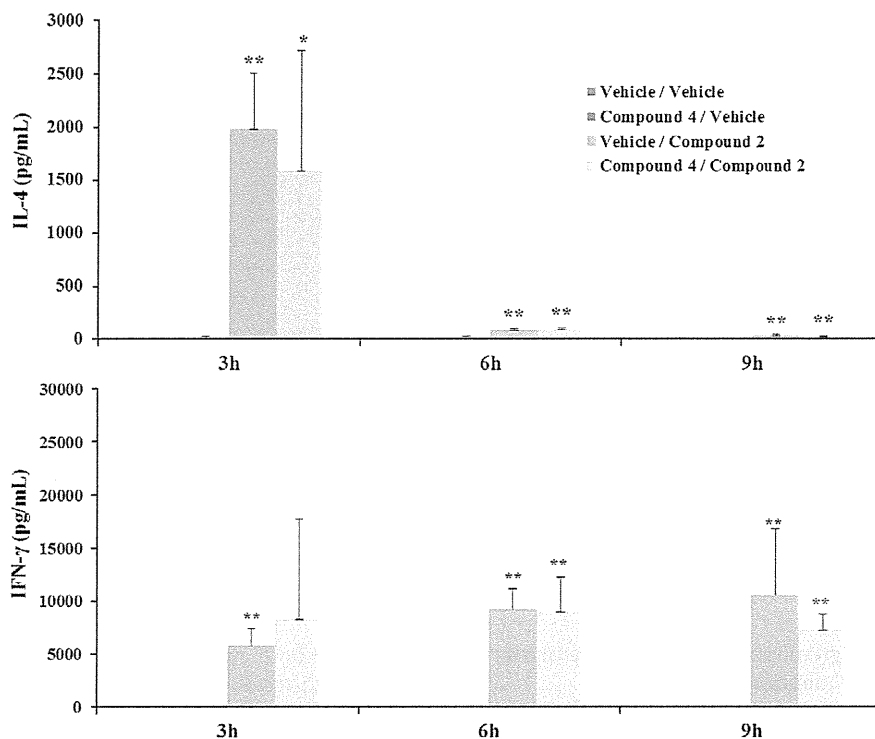
Figure 3. In vivo IL-4/IFN-γ production profile of **2** and **4** after iv administration to C57BL/6 mice. The data are expressed as mean ± SD (N = 4–5). **p <0.01, *p <0.05 compared with vehicle group (Student's t-test).

the crystal structure of **1**/hCD1d complex[12] was performed utilizing MAESTRO[25] program. Contrary to our expectation, the optimized structure of **2** in the complex had only a subtle, insignificant difference from **1** (Fig. 2). Some of the above derivatives were also calculated in silico, including aromatic derivative **11l** in expectation of aromatic interaction(s), but no significant difference was observed either (data not shown). No significant conformational change in the α1 and α2 helices of CD1d was observed in the minimization initiated from the X-ray structure. Molecular dynamics simulation might be more appropriate for the understanding of this exquisite signaling system.[13]

C-Glycoside derivative (**4**) of **2** was prepared and evaluated for its cytokine inducing profile. Conversion of **1** to its C-glycoside analog **3** is reported to lead to striking enhancement of activity in in vivo animal models of malaria and lung cancer.[8] It is the only example of the C-glycoside which is more potent than corresponding O-glycoside. C-Glycoside (**3**) is shown to somehow stimulate prolonged IL-12 secretion from dendritic cells, followed by prolonged IFN-γ stimulation from NK cells. Compound **4** did not show induction of either cytokines in vitro (Table 2), and in contrast to **3** did not elevate cytokine levels in vivo when administered intravenously to C57BL/6 mice (Fig. 3). In addition, **4** was co-administered intravenously with **2** to evaluate its antagonistic activity. Compound **4** did not antagonize the elevation of IL-4 or IFN-γ levels caused by **2** (Fig. 3). Although the anomeric oxygen does not participate in the hydrogen bond network in the ternary complex with CD1d and NKT T-cell receptor,[11] subtle difference from O to CH_2 was shown to have great influence on the signal transduction.

3. Conclusion

Several analogs related to **1** have been prepared to date, and many of them are equipotent to or even more potent than **1** in the aspect of IFN-γ secretion. In this study, a series of analogs based on **2** with altered ceramide moiety was prepared for its

Th2-biased response, and evaluated in the context of IL-4/IFN-γ ratio. Compound **2** in terms of chain length was shown to be one of the optimal compounds for the desired profile. First examples of phytosphingosine-modified analogs were discovered with non-linear hydrocarbon chain or ether linkage that show similar cytokine inducing profile to **2**. Expected aromatic interaction in the sphingosine chain may be of use in the future derivatization. Unprecedented C-glycoside of **2** was prepared and evaluated, which was shown to have no cytokine production effect in vitro or in vivo. In the course of this study, versatile syntheses were developed which allowed preparation of unprecedented derivatives and new findings on Th2 biased immunomodulation. The method and the possibility of structure modification proven in this study should allow future access to the analogs improved in their pharmacological and physicochemical properties.

4. Experimental

4.1. Chemistry

Proton nuclear magnetic resonance spectra (^{1}H NMR) and carbon nuclear magnetic resonance spectra (^{13}C NMR) were recorded on Brucker ARX-400 or Brucker Avance III (400 MHz) spectrometer in the indicated solvent. Chemical shifts (δ) are reported in parts per million relative to the internal standard tetramethylsilane. High-resolution mass spectra (HRMS) and fast atom bombardment (FAB) mass spectra were recorded on JEOL JMS-700 mass spectrometer. Electro-spray ionization (ESI) mass spectra were recorded on Agilent G1956A MSD spectrometer system. Other chemical reagents and solvents were purchased from Aldrich, Tokyo Kasei Kogyo, Wako Pure Chemical Industries, Kanto Kagaku or Nacalai tesque and used without purification. Flash column chromatography was performed using Merck Silica Gel 60 (230–400 mesh) or Purif-Pack® SI 30um supplied by Shoko Scientific. The experimental procedure for alkyl chain derivative **2** is reported

previously.[15] Exemplified procedure for aryl derivative **11l**, alkoxy derivative **11p** and C-glycoside **4**, along with compound data for all compounds **11a–11r** are described.

4.1.1. (2R,3R,4R)-1,3-O-Benzylidene-2-O-methanesulfonyl-5-phenyl-1,2,3,4-pentanetetrol (6l)

To a suspension of CuI (4.28 g, 22.5 mmol) in THF (45 ml) was added 1.06 M PhLi in THF (85 ml, 90.1 mmol) dropwise at −40 °C and the mixture was stirred for 1 h. A solution of **5** (5.01 g, 22.6 mmol) in THF (15 ml) was added via cannula, and the reaction was slowly allowed to warm to rt over 6 h. The reaction was quenched with satd NH_4Cl aq, extracted with EtOAc and washed twice with half-satd NH_4Cl aq. The organic layer was filtered through Celite, dried over Na_2SO_4 and concentrated. The precipitation formed was filtered and purified by silica gel column chromatography (CH_2Cl_2/MeOH; 3%) to give a colorless solid (6.47 g, 96%). To the solution of this diol (6.40 g, 21.3 mmol) in pyridine (70 ml) was added methanesulfonyl chloride (1.65 ml, 21.3 mmol) at 0 °C, and the mixture was gradually warmed to rt. Pyridine was removed under reduced pressure after consumption of the starting diol, and the residue was diluted with EtOAc, washed twice with water and brine, dried over Na_2SO_4 and concentrated. The residue was purified by silica gel column chromatography (hexane/EtOAc; 50%) to yield **6l** as a colorless solid (2.75 g, 34%). ¹H NMR (400 MHz, CDCl₃) δ = 7.55–7.52 (m, 2H), 7.44–7.20 (m, 8H), 5.59 (s, 1H), 4.91 (d, J = 1.3 Hz, 1H), 4.52 (dd, J = 1.5, 13.2 Hz, 1H), 4.12 (dd, J = 1.2, 13.3 Hz, 1H), 4.10–4.05 (m, 1H), 3.77 (dd, J = 1.2, 9.0 Hz, 1H), 3.18 (dd, J = 2.8, 13.9 Hz, 1H), 3.13 (s, 3H), 2.78 (dd, J = 7.7, 13.8 Hz, 1H), 2.61 (d, J = 5.2 Hz, 1H).

4.1.2. (2S,3S,4R)-2-Azido-3,4-O-isopropylidene-5-phenyl-1,3,4-pentanetriol (7l)

A mixture of **6l** (2.70 g, 7.14 mmol) and NaN₃ (5.57 g, 85.7 mmol) in DMF (35 ml) was stirred at 110 °C for 17 h. The reaction was diluted with EtOAc, washed with water and brine, dried over Na_2SO_4, and concentrated. The residue was purified by silica gel column chromatography (hexane/EtOAc; 40–66%) to yield the azide (892 mg, 38%). To this azide (860 mg, 2.65 mmol) in MeOH (14 ml) was added 6 N HCl (1.3 ml, 7.95 mmol) at 0 °C, and the mixture was stirred for 4 h. The reaction was neutralized with solid K_2CO_3, then filtered, concentrated and purified by silica gel column chromatography (hexane/EtOAc; 40–66%) to yield the triol (434 mg, 69%). The triol (430 mg, 1.81 mmol) was dissolved in 2,2-dimethoxypropane (7 ml), catalytic amount of p-toluenesulfonic acid monohydrate (174 mg, 0.092 mmol) was added, and the mixture was stirred for 2 h. MeOH was added and the reaction was stirred for 1 h. The mixture was concentrated and directly purified by silica gel column chromatography (hexane/EtOAc; 17%) to yield **7l** as a colorless oil (350 mg, 70%). ¹H NMR (400 MHz, CDCl₃) δ = 7.35–7.17 (m, 5H), 4.45 (ddd, J = 3.1, 5.6, 10.2 Hz, 1H), 4.12–4.00 (m, 2H), 3.98–3.88 (m, 1H), 3.65–3.55 (m, 1H), 3.01 (dd, J = 3.0, 14.1 Hz, 1H), 2.81 (dd, J = 10.4, 14.0 Hz, 1H), 2.07 (dd, J = 5.4, 6.8 Hz, 1H), 1.53 (s, 3H), 1.49 (s, 3H).

4.1.3. (2S,3S,4R)-2-Azido-3,4-O-isopropylidene-5-phenyl-1-O-(2,3,4,6-tetra-O-benzyl-α-D-galactosyl)-1,3,4-pentanetriol (9l)

To a mixture of **7l** (175 mg, 0.633 mmol), **8a** (446 mg, 0.822 mmol) and molecular sieves 4 Å in CHCl₃ (14 ml) under Ar was added dropwise at −50 °C a solution of $BF_3·OEt_2$ (80 μl, 0.631 mmol) in CHCl₃ (2.7 ml). After 1 h of stirring the reaction was quenched with satd NaHCO₃ aq, extracted with CH_2Cl_2, washed with brine, dried over Na_2SO_4 and purified by silica gel column chromatography (hexane/EtOAc; 12.5%) to give **9l** as a colorless oil (108 mg, 21%). ¹H NMR (400 MHz, CDCl₃) δ = 7.40–7.15 (m, 25H), 4.96 (d, J = 3.7 Hz, 1H), 4.95 (d, J = 11.2 Hz, 1H), 4.84 (d, J = 12.2 Hz, 1H), 4.81 (d, J = 13.0 Hz, 1H), 4.72 (d,

J = 11.8 Hz, 1H), 4.71 (d, J = 12.0 Hz, 1H), 4.57 (d, J = 11.5 Hz, 1H), 4.48 (d, J = 11.9 Hz, 1H), 4.41 (d, J = 12.1 Hz, 1H), 4.42–4.33 (m, 1H), 4.20–3.90 (m, 6H), 3.77 (dd, J = 6.5, 10.8 Hz, 1H), 3.65–3.45 (m, 3H), 3.00 (dd, J = 2.8, 14.1 Hz, 1H), 2.78 (dd, J = 10.5, 14.0 Hz, 1H), 1.44 (s, 3H), 1.23 (s, 3H).

4.1.4. (2S,3S,4R)-3,4-O-Isopropylidene-5-phenyl-1-O-(2,3,4,6-tetra-O-benzyl-α-D-galactosyl)-2-tetracosanoylamino-1,3,4-pentanetriol (10l)

A mixture of **9l** (98.2 mg, 0.123 mmol) and Lindlar catalyst (98 mg) in EtOH (5 ml) was stirred under H₂ atmosphere for 24 h. Additional Lindlar catalyst (96 mg) was added and the mixture was stirred for another 24 h. Insolubles were removed by filtration through membrane filter and the filtrate was concentrated to give an oil. The oil was diluted with CH_2Cl_2 (2 ml) and 1-ethyl-3-(3-dimethylaminopropyl) carbodiimide hydrochloride (26.8 mg, 0.140 mmol) was added. This mixture was added at 0 °C to the premixed suspension of Lignoceric acid (44.8 mg, 0.122 mmol), 1-hydroxybenzotrilazole (20.3 mg, 0.150 mmol) and Hunig's Base (49 μl, 0.281 mmol), in DMF (2.5 ml) and CH_2Cl_2 (5 ml), and the mixture was stirred at rt for 24 h. The reaction mixture was diluted with [Et₂O/EtOAc = 1:1] solution, quenched with satd NaHCO₃ aq, washed with 1 N HCl and brine, dried over Na_2SO_4, concentrated and purified by silica gel column chromatography (hexane/EtOAc; 25–33%) to give **10l** as a colorless solid (90.0 mg, 65% in two steps). ¹H NMR (400 MHz, CDCl₃) δ = 7.40–7.08 (m, 25H), 6.32 (d, J = 8.4 Hz, 1H), 4.924 (d, J = 11.4 Hz, 1H), 4.919 (d, J = 3.9 Hz, 1H), 4.82 (d, J = 11.4 Hz, 1H), 4.81 (d, J = 11.7 Hz, 1H), 4.74 (d, J = 11.7 Hz, 1H), 4.66 (d, J = 11.5 Hz, 1H), 4.58 (d, J = 11.6 Hz, 1H), 4.47 (d, J = 11.8 Hz, 1H), 4.37 (d, J = 11.8 Hz, 1H), 4.25–4.05 (m, 4H), 4.06 (dd, J = 3.3, 9.7 Hz, 1H), 3.98 (t, J = 6.1 Hz, 1H), 3.95–3.90 (m, 2H), 3.65 (d, J = 11.2 Hz, 1H), 3.55 (dd, J = 7.0, 9.5 Hz, 1H), 3.38 (dd, J = 5.6, 9.4 Hz, 1H), 2.75–2.70 (m, 2H), 2.18–1.93 (m, 2H), 1.60–1.50 (m, 2H), 1.47 (s, 3H), 1.28 (s, 3H), 1.35–1.20 (m, 40H), 0.87 (t, J = 6.5 Hz, 3H).

4.1.5. (2S,3S,4R)-1-O-(α-D-Galactosyl)-5-phenyl-2-tetracosanoylamino-1,3,4-pentanetriol (11l)

To a solution of **10l** (90.0 mg, 0.0801 mmol) in CH_2Cl_2 (5 ml) and MeOH (1 ml) was added 4 M HCl in dioxane (100 μl, 0.4 mmol) at 0 °C and the mixture was stirred at rt for 3 h. Silica gel was added to the reaction mixture, then volatiles were removed under reduced pressure. The residue was purified by silica gel column chromatography (hexane/EtOAc; 25–33%) to give a colorless solid (68 mg, 78%). A mixture of this solid (67 mg, 0.062 mmol) and Pearlman's catalyst (26.8 mg) in CHCl₃ (1 ml) and MeOH (3 ml) was stirred under H₂ atmosphere for 1.5 h. Insolubles were removed by filtration through membrane filter and the filtrate was concentrated to give compound **11l** as a colorless solid (43.6 mg, 98%). ¹H NMR (400 MHz, Pyr-d₅) δ = 8.53 (d, J = 8.8 Hz, 1H), 7.62 (d, J = 6.8 Hz, 2H), 7.32–7.27 (m, 2H), 7.20–7.17 (m, 1H), 6.83 (d, J = 4.6 Hz, 1H), 6.58–6.44 (m, 3H), 6.33 (d, J = 6.7 Hz, 1H), 6.27 (d, J = 4.0 Hz, 1H), 5.51 (d, J = 3.9 Hz, 1H), 5.27 (qd, J = 4.7, 8.9 Hz, 1H), 4.69–4.59 (m, 2H), 4.58–4.31 (m, 8H), 3.70 (dd, J = 1.8, 13.5 Hz, 1H), 3.14 (dd, J = 9.3, 13.7 Hz, 1H), 2.49–2.38 (m, 2H), 1.81 (quin, J = 7.5 Hz, 2H), 1.39–1.18 (m, 40H), 0.87 (t, J = 6.7 Hz, 3H); ¹³C NMR (101 MHz, Pyr-d₅) δ = 173.4, 130.5, 128.5, 101.8, 76.6, 74.0, 73.1, 71.6, 71.0, 70.4, 69.3, 62.7, 51.7, 40.7, 36.8, 32.1, 30.0, 30.0, 29.9, 29.9, 29.8, 29.6, 26.4, 23.0, 14.3; HRMS (FAB) Calcd for $C_{41}H_{73}NNaO_9^+$: 746.5178; Found: 746.5157.

4.1.6. (2R,3R,4R)-1,3-O-Benzylidene-2-O-methanesulfonyl-6-oxa-1,2,3,4-nonanetetrol (6p)

NaH (1.82 g, 45.4 mmol) was added to 1-propanol (60 ml) at 0 °C and stirred for 5 min. To the solution was added **5** (2.00 g, 9.01 mmol), and the mixture was stirred at rt for 20 h. To the reac-

tion mixture was added water (200 mL), and the product was extracted with EtOAc (200 mL × 1, 50 ml × 2). The combined organic layer was dried over Na_2SO_4, filtered, concentrated and purified over silica gel column chromatography (hexane/EtOAc; 50–67%) to yield the ether as a colorless solid (2.12 g, 83%). To the solution of above ether (451 mg, 1.60 mmol) in pyridine (15 ml) was added methanesulfonyl chloride (118 μl, 1.51 mmol) at −40 °C, and the mixture was gradually warmed to rt. After 36 h of stirring pyridine was removed azeotropically with heptane. The residue was directly purified by column chromatography (hexane/EtOAc; 40–66%) to yield **6p** as a colorless solid (357.0 mg, 62%). ^{1}H NMR (400 MHz, CDCl$_3$) δ = 7.52–7.44 (m, 2H), 7.41–7.35 (m, 3H), 5.58 (s, 1H), 4.88 (dd, J = 1.5, 3.0 Hz, 1H), 4.59 (dd, J = 1.6, 13.2 Hz, 1H), 4.16 (dd, J = 1.3, 13.2 Hz, 1H), 4.04 (dd, J = 1.5, 9.2 Hz, 1H), 4.00–3.93 (m, 1H), 3.67 (dd, J = 2.9, 9.8 Hz, 1H), 3.63 (dd, J = 4.4, 9.8 Hz, 1H), 3.47 (ddd, J = 6.7, 9.5, 13.8 Hz, 2H), 3.17 (s, 3H), 2.76 (d, J = 6.4 Hz, 1H), 1.61 (sxt, J = 7.1 Hz, 2H), 0.93 (t, J = 7.5 Hz, 3H); MS (ESI) 361.1 (M+H)$^+$.

4.1.7. (2*S*,3*S*,4*R*)-2-Azido-3,4-*O*-isopropylidene-6-oxa-1,3,4-nonanetriol (7p)

A mixture of **6p** (325 mg, 0.901 mmol) and Pearlman's catalyst (61.3 mg, 0.437 mmol) in EtOH (10 ml) was stirred under H$_2$ atmosphere at rt for 90 min. Insolubles were removed by filtration through membrane filter and the filtrate was concentrated to give a colorless oil which contained EtOH (281.3 mg, calculated from ^{1}H NMR to contain 242 mg of the triol, 99%). EtOAc was added and removed under reduced pressure repeatedly for three times to remove EtOH. The residue was dissolved in DMF (5 ml), NaN$_3$ (236 mg, 3.63 mmol) was added and the mixture was stirred under Ar at 95 °C for 3 h. To the reaction mixture was added half-satd NaHCO$_3$ (100 mL), and the product was extracted with EtOAc (100 mL × 1, 50 ml × 8). The combined organic layer was dried over Na$_2$SO$_4$, filtered, concentrated and purified by silica gel column chromatography ([hexane/EtOAc = 1:1]/MeOH; 2–5%) to give the azido-triol as a colorless oil (119.0 mg, 60%). The residue was dissolved in 2,2-dimethoxypropane (2 ml), catalytic amount of *p*-toluenesulfonic acid monohydrate (5 mg, 0.026 mmol) was added at 0 °C, and the mixture was stirred for 21 h during which ice in the cooling bath gradually melted. MeOH was added and the reaction was stirred for 2 h. To the mixture was added half-satd NaHCO$_3$ aq (75 mL), and the product was extracted with EtOAc (75 mL × 1, 40 ml × 2). The combined organic layer was dried over Na$_2$SO$_4$, filtered, concentrated and purified by silica gel column chromatography (hexane/EtOAc; 20–50%, then to [hexane/EtOAc = 1:1]/MeOH; 5%) to yield **7p** as a colorless oil (36.9 mg, 26%). ^{1}H NMR (400 MHz, DMSO-d_6) δ = 5.10 (br s, 1H), 4.23 (q, J = 5.8 Hz, 1H), 3.93 (dd, J = 5.9, 9.0 Hz, 1H), 3.80 (dd, J = 1.5, 11.0 Hz, 1H), 3.62 (dd, J = 5.0, 10.5 Hz, 1H), 3.60–3.49 (m, 2H), 3.46 (dd, J = 5.8, 10.5 Hz, 1H), 3.39 (t, J = 6.7 Hz, 2H), 1.53 (sxt, J = 7.1 Hz, 2H), 1.34 (s, 3H), 1.25 (s, 3H), 0.87 (t, J = 7.4 Hz, 3H); ^{13}C NMR (101 MHz, DMSO-d_6) δ = 107.8, 75.6, 74.5, 72.3, 68.7, 62.2, 61.6, 27.4, 25.2, 22.2, 10.4; MS (ESI) 232.2 (M−N$_2$+H)$^+$.

4.1.8. (2*S*,3*S*,4*R*)-2-Azido-3,4-*O*-isopropylidene-6-oxa-1-*O*-(2,3,4,6-tetra-*O*-benzyl-α-D-galactosyl)-1,3,4-nonanetriol (9p)

To a solution of **7p** (36.9 mg, 0.142 mmol) in toluene (3 ml) under Ar were added molecular sieves 4 Å (151.3 mg), a solution of tetra-*O*-benzyl-galactosyl chloride **8b** (162 mg, 0.29 mmol) in toluene (7 ml), tetra-*n*-butylammonium bromide (140.9 mg, 0.437 mmol) and Hunig's Base (50 μl, 0.286 mmol) at rt. The mixture was stirred at rt for 45 min, at 60 °C for 45 h, and at 80 °C for 15 h. MeOH was added at 50 °C and stirred for 6 h. The reaction mixture was passed through Celite pad to remove insolubles, and to the filtrate was added half-satd NaHCO$_3$ aq (100 ml). The product was extracted with EtOAc (100 ml × 1, 50 ml × 1), and the

combined organic layer was dried over Na$_2$SO$_4$, filtered, concentrated and subjected to silica gel column chromatography (hexane/EtOAc; 11% to 14%) to give **9p** as a colorless oil (98.0 mg) as a mixture with tetra-*O*-benzyl-1-methoxygalactose. Tetra-*O*-benzyl-1-methoxygalactose was removed in the next step. MS (FAB) 804 (M+Na)$^+$.

4.1.9. (2*S*,3*S*,4*R*)-3,4-*O*-Isopropylidene-6-oxa-1-*O*-(2,3,4,6-tetra-*O*-benzyl-α-D-galactosyl)-2-tetracosanoylamino-1,3,4-nonanetriol (10p)

The crude **9p** obtained in 4.1.8 was divided into two portions. One portion was dissolved in EtOH (3 ml) and stirred with Lindlar catalyst (20.8 mg) under H$_2$ atmosphere for 22 h. Insolubles were removed by filtration through membrane filter and the filtrate was concentrated to give an oil. The oil was diluted with CH$_2$Cl$_2$ (1 ml) and DMF (1 ml), and to the solution was added premixed suspension of Lignoceric acid (10.5 mg, 0.028 mmol), 3*H*-[1,2,3]-triazolo[4,5-*b*]pyridin-3-ol (4.5 mg, 0.033 mmol) and 1-ethyl-3-(3-dimethylaminopropyl) carbodiimide hydrochloride (7.4 mg, 0.039 mmol) in DMF (1 ml) and CH$_2$Cl$_2$ (1 ml), then Hunig's Base (12 μl, 0.069 mmol), and the mixture was stirred at 35 °C for 17 h. To the reaction mixture was added half-satd NaHCO$_3$ aq (100 mL), and the product was extracted with [hexane/EtOAc = 1:1] solution (100 mL × 1, 50 ml × 2). The combined organic layer was dried over Na$_2$SO$_4$, filtered, concentrated and purified by silica gel column chromatography (hexane/EtOAc; 25%) to give **10p** as colorless oil (17.8 mg). The same procedure was applied to the other portion of the crude **9p**, and the products from both portions were combined to yield 35.1 mg (22% from **7p**) as a colorless oil. ^{1}H NMR (400 MHz, CDCl$_3$) δ = 7.42–7.19 (m, 20H), 6.36 (d, J = 9.4 Hz, 1H), 4.93 (d, J = 11.5 Hz, 1H), 4.89 (d, J = 3.8 Hz, 1H), 4.81 (d, J = 11.4 Hz, 1H), 4.80 (d, J = 11.4 Hz, 1H), 4.74 (d, J = 11.7 Hz, 1H), 4.66 (d, J = 11.5 Hz, 1H), 4.58 (d, J = 11.5 Hz, 1H), 4.48 (d, J = 11.8 Hz, 1H), 4.38 (d, J = 11.9 Hz, 1H), 4.23–4.02 (m, 5H), 3.98–3.88 (m, 3H), 3.61 (dd, J = 2.6, 11.4 Hz, 1H), 3.54 (dd, J = 6.8, 9.3 Hz, 1H), 3.45–3.34 (m, 4H), 3.30 (td, J = 7.0, 9.4 Hz, 1H), 2.10–1.94 (m, 2H), 1.61–1.52 (m, 4H), 1.44 (s, 3H), 1.33 (s, 3H), 1.32–1.19 (m, 40H), 0.88 (t, J = 7.2 Hz, 3H), 0.87 (t, J = 7.3 Hz, 3H); ^{13}C NMR (101 MHz, CDCl$_3$) δ = 138.3, 128.5, 128.4, 128.4, 128.3, 128.3, 128.0, 127.9, 127.7, 127.6, 127.5, 108.7, 99.6, 78.9, 74.7, 74.6, 73.5, 73.4, 73.0, 36.8, 31.9, 29.7, 29.7, 29.6, 29.4, 29.4, 25.8, 25.6, 22.7, 14.1, 10.4; MS (FAB) 1128 (M+Na−1)$^+$.

4.1.10. (2*S*,3*S*,4*R*)-1-*O*-(α-D-Galactosyl)-6-oxa-2-tetracosanoylamino-1,3,4-nonanetriol (11p)

To a solution of **10p** (16.4 mg, 0.015 mmol) in CH$_2$Cl$_2$ (4 ml) and MeOH (0.8 ml) was added 4 M HCl in dioxane (80 μl, 0.320 mmol) and the mixture was stirred at rt for 2 h. Et$_3$N (90 μl, 0.646 mmol) was added, then volatiles were removed under reduced pressure to give solid, which was purified by silica gel column chromatography (hexane/EtOAc; 33% to 44%) to give colorless solid (13.8 mg, 87%). A mixture of above solid (12.5 mg, 0.012 mmol) and Pearlman's catalyst (7.5 mg) in CH$_2$Cl$_2$ (1 ml) and MeOH (3 ml) was stirred under H$_2$ atmosphere for 3.5 h. Insolubles were removed by filtration through membrane filter and the filtrate was concentrated to give compound **11p** as a colorless solid (8.8 mg, quant.) ^{1}H NMR (400 MHz, Pyr-d_5) δ = 8.45 (d, J = 8.7 Hz, 1H), 6.86 (d, J = 6.7 Hz, 1H), 6.53 (d, J = 6.1 Hz, 1H), 6.50–6.41 (m, 2H), 6.34 (d, J = 6.4 Hz, 1H), 6.27 (d, J = 4.1 Hz, 1H), 5.54 (d, J = 3.8 Hz, 1H), 5.30–5.21 (m, 1H), 4.69–4.59 (m, 2H), 4.57–4.53 (m, 1H), 4.53–4.34 (m, 7H), 4.12 (dd, J = 2.7, 9.9 Hz, 1H), 3.99 (dd, J = 6.0, 9.9 Hz, 1H), 3.45 (tq, J = 6.7, 9.1 Hz, 2H), 2.42 (dt, J = 1.8, 7.5 Hz, 2H), 1.79 (quin, J = 7.5 Hz, 2H), 1.54 (sxt, J = 7.1 Hz, 2H), 1.39–1.15 (m, 40H), 0.87 (t, J = 6.8 Hz, 3H), 0.82 (t, J = 7.5 Hz, 3H); ^{13}C NMR (101 MHz, Pyr-d_5) δ = 173.4, 101.6, 74.2, 74.1, 73.3, 73.1, 72.1, 71.7, 71.0, 70.4, 68.7, 62.7, 51.6, 36.8, 32.1, 30.0, 30.0, 29.9, 29.9, 29.8, 29.8, 29.6,

26.4, 23.3, 23.0, 14.3, 10.8; HRMS (FAB) Calcd for $C_{38}H_{75}NNaO_{10}^+$: 728.5283; Found: 728.5311.

4.1.11. (2S,3S,4R)-1-O-(α-D-Galactosyl)-2-tetracosanoylamino-1,3,4-heptanetriol (11a)

^{1}H NMR (400 MHz, Pyr-d_5) δ = 8.40 (d, J = 8.5 Hz, 1H), 6.91 (d, J = 6.1 Hz, 1H), 6.59 (d, J = 6.1 Hz, 1H), 6.48 (t, J = 5.6 Hz, 1H), 6.38 (d, J = 6.1 Hz, 1H), 6.26 (d, J = 3.9 Hz, 1H), 6.03 (d, J = 5.9 Hz, 1H), 5.57 (d, J = 3.8 Hz, 1H), 5.30–5.21 (m, 1H), 4.70–4.61 (m, 2H), 4.58–4.53 (m, 1H), 4.53–4.47 (m, 1H), 4.47–4.34 (m, 4H), 4.33–4.23 (m, 2H), 2.43 (t, J = 7.5 Hz, 2H), 2.27–2.14 (m, 1H), 1.94–1.75 (m, 4H), 1.74–1.57 (m, 1H), 1.41–1.14 (m, 40H), 0.96 (t, J = 7.3 Hz, 3H), 0.87 (t, J = 6.9 Hz, 3H); ^{13}C NMR (101 MHz, Pyr-d_5) δ = 173.2, 101.6, 76.9, 73.1, 72.2, 71.7, 71.0, 70.3, 68.7, 62.7, 51.4, 36.8, 36.6, 32.1, 30.0, 30.0, 29.9, 29.9, 29.8, 29.8, 29.6, 26.4, 23.0, 19.6, 14.6, 14.3; HRMS (FAB) Calcd for $C_{37}H_{73}NNaO_9^+$: 698.5178; Found: 698.5151.

4.1.12. (2S,3S,4R)-1-O-(α-D-Galactosyl)-2-tricosanoylamino-1,3,4-octanetriol (11b)

^{1}H NMR (400 MHz, Pyr-d_5) δ = 8.42 (d, J = 8.7 Hz, 1H), 5.57 (d, J = 3.8 Hz, 1H), 5.31–5.21 (m, 1H), 4.70–4.62 (m, 2H), 4.58–4.54 (m, 1H), 4.54–4.48 (m, 1H), 4.46–4.35 (m, 4H), 4.32–4.24 (m, 2H), 2.44 (t, J = 7.2 Hz, 2H), 2.32–2.17 (m, 1H), 1.90–1.74 (m, 4H), 1.70–1.53 (m, 1H), 1.46–1.16 (m, 40H), 0.91–0.80 (m, 6H); ^{13}C NMR (101 MHz, Pyr-d_5) δ = 173.3, 101.6, 76.8, 73.1, 72.5, 71.6, 71.1, 70.3, 68.7, 62.7, 51.4, 36.8, 34.1, 32.1, 30.0, 29.9, 29.9, 29.8, 29.8, 29.6, 28.6, 26.4, 23.3, 23.0, 14.4, 14.3; HRMS (FAB) Calcd for $C_{37}H_{73}NNaO_9^+$: 698.5178; Found: 698.5161.

4.1.13. (2S,3S,4R)-1-O-(α-D-Galactosyl)-2-tetracosanoylamino-1,3,4-octanetriol (11c)

^{1}H NMR (400 MHz, Pyr-d_5) δ = 8.41 (d, J = 8.7 Hz, 1H), 6.96–6.86 (m, 1H), 6.65–6.53 (m, 1H), 6.53–6.43 (m, 1H), 6.37 (d, J = 6.1 Hz, 1H), 6.31–6.20 (m, 1H), 6.03 (d, J = 5.1 Hz, 1H), 5.57 (d, J = 3.9 Hz, 1H), 5.31–5.21 (m, 1H), 4.71–4.62 (m, 2H), 4.55 (br s, 1H), 4.53–4.48 (m, 1H), 4.47–4.35 (m, 4H), 4.32–4.22 (m, 2H), 2.43 (t, J = 7.2 Hz, 2H), 2.32–2.18 (m, 1H), 1.91–1.72 (m, 4H), 1.67–1.53 (m, 1H), 1.47–1.15 (m, 42H), 0.87 (t, J = 6.8 Hz, 3 H), 0.85 (t, J = 6.9 Hz, 3H); ^{13}C NMR (101 MHz, Pyr-d_5) δ = 173.2, 101.6, 76.9, 73.1, 72.5, 71.7, 71.1, 70.3, 68.7, 62.7, 51.4, 36.8, 34.1, 32.1, 30.0, 30.0, 29.9, 29.9, 29.8, 29.8, 29.6, 28.6, 26.4, 23.3, 23.0, 14.4, 14.3; HRMS (FAB) Calcd for $C_{38}H_{75}NNaO_9^+$: 712.5334; Found: 712.5316.

4.1.14. (2S,3S,4R)-1-O-(α-D-Galactosyl)-2-icosanoylamino-1,3,4-nonanetriol (11d)

^{1}H NMR (400 MHz, Pyr-d_5) δ = 8.42 (d, J = 8.7 Hz, 1H), 6.91 (d, J = 6.4 Hz, 1H), 6.57 (d, J = 4.8 Hz, 1H), 6.49 (t, J = 5.5 Hz, 1H), 6.39 (d, J = 6.1 Hz, 1H), 6.26 (d, J = 3.6 Hz, 1H), 6.03 (d, J = 5.8 Hz, 1H), 5.57 (d, J = 3.9 Hz, 1H), 5.30–5.21 (m, 1H), 4.71–4.61 (m, 2H), 4.55 (br s, 1H), 4.53–4.48 (m, 1H), 4.47–4.35 (m, 4H), 4.34–4.23 (m, 2H), 2.44 (t, J = 7.2 Hz, 2H), 2.30–2.17 (m, 1H), 1.93–1.74 (m, 4H), 1.70–1.56 (m, 1H), 1.41–1.15 (m, 36H), 0.87 (t, J = 6.8 Hz, 3H), 0.81 (t, J = 7.0 Hz, 3H); ^{13}C NMR (101 MHz, Pyr-d_5) δ = 173.3, 101.6, 76.8, 73.1, 72.5, 71.7, 71.0, 70.4, 68.7, 62.7, 51.5, 36.8, 34.4, 32.5, 32.1, 30.0, 30.0, 29.9, 29.9, 29.8, 29.8, 29.6, 26.4, 26.1, 23.0, 23.0, 14.3, 14.3; HRMS (FAB) Calcd for $C_{35}H_{69}NNaO_{9+}$: 670.4865; Found: 670.4880.

4.1.15. (2S,3S,4R)-1-O-(α-D-Galactosyl)-2-docosanoylamino-1,3,4-nonanetriol (11e)

^{1}H NMR (400 MHz, Pyr-d_5) δ = 8.42 (d, J = 8.7 Hz, 1H), 6.90 (br s, 1H), 6.57 (d, J = 4.4 Hz, 1H), 6.49 (t, J = 5.3 Hz, 1H), 6.39 (d, J = 5.9 Hz, 1H), 6.26 (d, J = 3.9 Hz, 1H), 6.03 (d, J = 5.5 Hz, 1H), 5.57 (d, J = 3.8 Hz, 1H), 5.31–5.20 (m, 1H), 4.71–4.61 (m, 2H),

4.55 (br s, 1H), 4.53–4.48 (m, 1H), 4.47–4.36 (m, 4H), 4.33–4.24 (m, 2H), 2.44 (t, J = 7.2 Hz, 2H), 2.30–2.18 (m, 1H), 1.93–1.75 (m, 4H), 1.70–1.54 (m, 1H), 1.45–1.11 (m, 40H), 0.87 (t, J = 6.8 Hz, 3H), 0.81 (t, J = 7.0 Hz, 3H); ^{13}C NMR (101 MHz, Pyr-d_5) δ = 173.3, 101.6, 76.8, 73.1, 72.5, 71.7, 71.1, 70.4, 68.7, 62.7, 51.5, 36.8, 34.4, 32.5, 32.1, 30.0, 30.0, 29.9, 29.9, 29.8, 29.8, 29.6, 26.4, 26.1, 23.0, 23.0, 14.3, 14.3; HRMS (FAB) Calcd for $C_{37}H_{73}NNaO_9^+$: 698.5178; Found: 698.5145.

4.1.16. (2S,3S,4R)-1-O-(α-D-Galactosyl)-2-tricosanoylamino-1,3,4-nonanetriol (11f)

^{1}H NMR (400 MHz, Pyr-d_5) δ = 8.42 (d, J = 8.5 Hz, 1H), 5.58 (d, J = 3.9 Hz, 1H), 5.30–5.22 (m, 1H), 4.71–4.62 (m, 2H), 4.58–4.54 (m, 1H), 4.54–4.49 (m, 1H), 4.47–4.36 (m, 4H), 4.33–4.25 (m, 2H), 2.44 (t, J = 7.3 Hz, 2H), 2.31–2.18 (m, 1H), 1.94–1.76 (m, 4H), 1.69–1.56 (m, 1H), 1.41–1.18 (m, 42H), 0.87 (t, J = 6.9 Hz, 3H), 0.81 (t, J = 7.2 Hz, 3H); ^{13}C NMR (101 MHz, Pyr-d_5) δ = 101.6, 76.8, 73.1, 72.5, 71.7, 71.0, 70.3, 62.7, 51.5, 36.8, 34.4, 32.5, 32.1, 30.0, 29.9, 29.8, 29.6, 26.4, 26.1, 23.0, 23.0, 14.3, 14.3; HRMS (FAB) Calcd for $C_{38}H_{75}NNaO_9^+$: 712.5334; Found: 712.5302.

4.1.17. (2S,3S,4R)-1-O-(α-D-Galactosyl)-2-pentacosanoylamino-1,3,4-nonanetriol (11g)

^{1}H NMR (400 MHz, Pyr-d_5) δ = 8.43 (d, J = 8.7 Hz, 1H), 6.92 (d, J = 4.0 Hz, 1H), 6.58 (d, J = 3.6 Hz, 1H), 6.50 (t, J = 5.3 Hz, 1H), 6.40 (d, J = 6.0 Hz, 1H), 6.27 (d, J = 3.4 Hz, 1H), 6.03 (d, J = 5.6 Hz, 1H), 5.58 (d, J = 3.8 Hz, 1H), 5.32–5.20 (m, 1H), 4.71–4.61 (m, 2H), 4.55 (br s, 1H), 4.54–4.48 (m, 1H), 4.47–4.35 (m, 4H), 4.29 (br s, 2H), 2.44 (t, J = 7.3 Hz, 2H), 2.30–2.18 (m, 1H), 1.94–1.75 (m, 4H), 1.70–1.56 (m, 1H), 1.38–1.20 (m, 46H), 0.87 (t, J = 6.8 Hz, 3H), 0.81 (t, J = 7.1 Hz, 3H); ^{13}C NMR (101 MHz, Pyr-d_5) δ = 173.3, 101.6, 76.8, 73.1, 72.5, 71.7, 71.0, 70.4, 68.7, 62.7, 51.5, 36.8, 34.4, 32.5, 32.1, 30.1, 30.0, 29.9, 29.9, 29.8, 29.8, 29.6, 26.4, 26.1, 23.0, 23.0, 14.3, 14.3; HRMS (FAB) Calcd for $C_{40}H_{79}NNaO_9^+$: 740.5647; Found: 740.5618.

4.1.18. (2S,3S,4R)-1-O-(α-D-Galactosyl)-2-hexacosanoylamino-1,3,4-nonanetriol (11h)

^{1}H NMR (400 MHz, Pyr-d_5) δ = 8.43 (d, J = 8.7 Hz, 1H), 6.92 (br s, 1H), 6.58 (br s, 1H), 6.49 (br s, 1H), 6.39 (d, J = 5.9 Hz, 1H), 6.27 (br s, 1H), 6.03 (d, J = 4.5 Hz, 1H), 5.58 (d, J = 3.9 Hz, 1H), 5.30–5.22 (m, 1H), 4.71–4.62 (m, 2H), 4.55 (br s, 1H), 4.54–4.48 (m, 1H), 4.48–4.34 (m, 4H), 4.33–4.24 (m, 2H), 2.44 (t, J = 7.2 Hz, 2H), 2.31–2.18 (m, 1H), 1.94–1.76 (m, 4H), 1.70–1.55 (m, 1H), 1.42–1.16 (m, 48H), 0.87 (t, J = 6.9 Hz, 3H), 0.81 (t, J = 7.1 Hz, 3H); ^{13}C NMR (101 MHz, Pyr-d_5) δ = 173.3, 101.6, 76.8, 73.1, 72.5, 71.7, 71.0, 70.4, 68.7, 62.7, 51.5, 36.8, 34.4, 32.5, 32.1, 30.1, 30.0, 29.9, 29.9, 29.8, 29.8, 29.6, 26.4, 26.1, 23.0, 23.0, 14.3; HRMS (FAB) Calcd for $C_{41}H_{81}NNaO_9^+$: 754.5804; Found: 754.5757.

4.1.19. (2S,3S,4R)-1-O-(α-D-Galactosyl)-2-octacosanoylamino-1,3,4-nonanetriol (11i)

^{1}H NMR (400 MHz, Pyr-d_5) δ = 8.42 (d, J = 8.7 Hz, 1H), 6.90 (d, J = 4.1 Hz, 1H), 6.57 (d, J = 4.9 Hz, 1H), 6.49 (t, J = 5.3 Hz, 1H), 6.39 (d, J = 6.1 Hz, 1H), 6.26 (d, J = 3.5 Hz, 1H), 6.02 (d, J = 5.6 Hz, 1H), 5.57 (d, J = 3.9 Hz, 1H), 5.30–5.20 (m, 1H), 4.71–4.61 (m, 2H), 4.57–4.48 (m, 2H), 4.47–4.36 (m, 4H), 4.33–4.25 (m, 2H), 2.44 (t, J = 7.2 Hz, 2H), 2.30–2.19 (m, 1H), 1.93–1.77 (m, 4H), 1.69–1.56 (m, 1H), 1.38–1.22 (m, 52H), 0.87 (t, J = 6.8 Hz, 3H), 0.81 (t, J = 7.1 Hz, 3H); ^{13}C NMR (101 MHz, Pyr-d_5) δ = 173.3, 101.6, 76.8, 73.1, 72.5, 71.7, 71.0, 70.4, 68.7, 62.7, 51.5, 36.8, 34.4, 32.5, 32.1, 30.1, 30.0, 29.9, 29.9, 29.8, 29.8, 29.6, 26.4, 26.1, 23.0, 23.0, 14.3, 14.3; HRMS (FAB) Calcd for $C_{43}H_{85}NNaO_9^+$: 782.6117; Found: 782.6116.

4.1.20. (2S,3S,4R)-1-O-(α-D-Galactosyl)-2-tricosanoylamino-1,3,4-decanetriol (11j)

^{1}H NMR (400 MHz, Pyr-d_5) δ = 8.43 (d, J = 8.7 Hz, 1H), 6.92 (d, J = 6.3 Hz, 1H), 6.58 (d, J = 6.0 Hz, 1H), 6.49 (t, J = 5.6 Hz, 1H), 6.40 (d, J = 6.1 Hz, 1H), 6.27 (d, J = 4.0 Hz, 1H), 6.04 (d, J = 5.9 Hz, 1H), 5.58 (d, J = 3.9 Hz, 1H), 5.31–5.21 (m, 1H), 4.71–4.61 (m, 2H), 4.58–4.54 (m, 1H), 4.54–4.49 (m, 1H), 4.47–4.35 (m, 4H), 4.34–4.25 (m, 2H), 2.44 (t, J = 7.2 Hz, 2H), 2.31–2.19 (m, 1H), 1.94–1.75 (m, 4H), 1.70–1.57 (m, 1H), 1.44–1.16 (m, 44H), 0.87 (t, J = 6.8 Hz, 3H), 0.80 (t, J = 7.1 Hz, 3H); ^{13}C NMR (101 MHz, Pyr-d_5) δ = 173.3, 101.6, 76.8, 73.1, 72.5, 71.7, 71.1, 70.4, 68.7, 62.7, 51.5, 36.8, 34.4, 32.2, 32.1, 30.1, 30.0, 29.9, 29.9, 29.8, 29.8, 29.6, 26.4, 23.0, 22.9, 14.3, 14.3; HRMS (FAB) Calcd for C$_{39}$H$_{77}$NNaO$_9$$^+$: 726.5491; Found: 726.5509.

4.1.21. (2S,3S,4R)-5-Cyclopentyl-1-O-(α-D-galactosyl)-2-tetracosanoylamino-1,3,4-pentanetriol (11k)

^{1}H NMR (400 MHz, Pyr-d_5) δ = 8.41 (d, J = 8.7 Hz, 1H), 6.91 (d, J = 4.9 Hz, 1H), 6.60 (d, J = 4.3 Hz, 1H), 6.49 (t, J = 5.5 Hz, 1H), 6.37 (d, J = 6.4 Hz, 1H), 6.26 (d, J = 3.9 Hz, 1H), 5.97 (d, J = 6.5 Hz, 1H), 5.57 (d, J = 3.9 Hz, 1H), 5.29–5.19 (m, 1H), 4.71–4.61 (m, 2H), 4.56 (br s, 1H), 4.54–4.49 (m, 1H), 4.47–4.25 (m, 6H), 2.51–2.35 (m, 3H), 2.20–2.11 (m, 1H), 2.01–1.88 (m, 2H), 1.88–1.76 (m, 3H), 1.61–1.49 (m, 2H), 1.49–1.16 (m, 44H), 0.87 (t, J = 6.9 Hz, 3H); ^{13}C NMR (101 MHz, Pyr-d_5) δ = 173.2, 101.6, 77.2, 73.1, 71.7, 71.1, 70.4, 68.7, 62.7, 51.4, 37.3, 36.8, 34.1, 32.4, 32.1, 30.0, 30.0, 29.9, 29.9, 29.8, 29.8, 29.6, 26.4, 25.5, 25.4, 23.0, 14.3; HRMS (FAB) Calcd for C$_{40}$H$_{77}$NNaO$_9$$^+$: 738.5491; Found: 738.5444.

4.1.22. (2S,3S,4R)-1-O-(α-D-Galactosyl)-6-phenyl-2-tetracosanoylamino-1,3,4-hexanetriol (11m)

^{1}H NMR (400 MHz, Pyr-d_5) δ = 8.35 (d, J = 8.7 Hz, 1H), 7.38–7.27 (m, 4H), 7.20–7.17 (m, 1H), 7.05 (br s, 1H), 6.59 (br s, 1H), 6.52–6.41 (m, 2H), 6.29 (br s, 1H), 6.22 (d, J = 5.9 Hz, 1H), 5.57 (d, J = 3.8 Hz, 1H), 5.31–5.22 (m, 1H), 4.69–4.59 (m, 2H), 4.56 (br s, 1H), 4.48–4.25 (m, 7H), 3.21 (ddd, J = 4.5, 9.8, 13.9 Hz, 1H), 3.00 (ddd, J = 6.8, 9.7, 13.5 Hz, 1H), 2.66–2.55 (m, 1H), 2.47–2.33 (m, 2H), 2.23–2.10 (m, 1H), 1.80 (quin, J = 7.6 Hz, 2H), 1.40–1.14 (m, 40H), 0.87 (t, J = 6.9 Hz, 3H); ^{13}C NMR (101 MHz, Pyr-d_5) δ = 173.2, 143.6, 129.1, 128.7, 125.9, 101.5, 76.8, 73.0, 71.7, 71.6, 71.0, 70.3, 68.4, 62.7, 51.3, 36.8, 36.5, 32.7, 32.1, 30.0, 29.9, 29.9, 29.8, 29.8, 29.6, 26.4, 23.0, 14.3; HRMS (FAB) Calcd for C$_{42}$H$_{75}$NNaO$_9$$^+$: 760.5334; Found: 760.5322.

4.1.23. (2S,3S,4R)-1-O-(α-D-Galactosyl)-5-(p-tolyl)-2-tetracosanoylamino-1,3,4-pentanetriol (11n)

^{1}H NMR (400 MHz, Pyr-d_5) δ = 8.51 (d, J = 8.5 Hz, 1H), 7.51 (d, J = 8.0 Hz, 2H), 7.08 (d, J = 7.7 Hz, 2H), 6.92–6.12 (m, 6H), 5.52 (d, J = 4.0 Hz, 1H), 5.28 (qd, J = 4.7, 8.9 Hz, 1H), 4.71–4.58 (m, 2H), 4.58–4.47 (m, 3H), 4.47–4.30 (m, 5H), 3.67 (dd, J = 1.8, 13.5 Hz, 1H), 3.12 (dd, J = 9.2, 13.8 Hz, 1H), 2.43 (dt, J = 3.3, 7.5 Hz, 2H), 2.21 (s, 3H), 1.81 (quin, J = 7.6 Hz, 2H), 1.43–1.10 (m, 40H), 0.87 (t, J = 6.8 Hz, 3H); ^{13}C NMR (101 MHz, Pyr-d_5) δ = 173.4, 138.2, 130.3, 129.1, 101.8, 76.5, 74.1, 73.1, 71.6, 71.0, 70.4, 69.2, 62.7, 51.7, 36.8, 32.1, 30.1, 30.0, 29.9, 29.9, 29.8, 29.8, 29.6, 26.4, 23.0, 21.0, 14.3; HRMS (FAB) Calcd for C$_{42}$H$_{75}$NNaO$_9$$^+$: 760.5334; Found: 760.5358.

4.1.24. (2S,3S,4R)-1-O-(α-D-Galactosyl)-6-oxa-2-tetracosanoylamino-1,3,4-heptanetriol (11o)

^{1}H NMR (400 MHz, Pyr-d_5) δ = 8.47 (d, J = 8.7 Hz, 1H), 5.54 (d, J = 3.9 Hz, 1H), 5.30–5.22 (m, 1H), 4.69–4.61 (m, 2H), 4.57–4.47 (m, 3H), 4.46–4.33 (m, 5H), 4.07 (dd, J = 2.7, 9.9 Hz, 1H), 3.94 (dd, J = 6.1, 9.8 Hz, 1H), 3.35 (s, 3H), 2.42 (dt, J = 1.5, 7.5 Hz, 2H), 1.79 (quin, J = 7.5 Hz, 2H), 1.38–1.14 (m, 40H), 0.87 (t, J = 7.0 Hz, 3H); ^{13}C NMR (101 MHz, Pyr-d_5) δ = 173.4, 101.6, 76.0, 74.0, 73.1, 72.0,

71.6, 71.0, 70.3, 68.5, 62.7, 59.0, 51.5, 36.8, 32.1, 30.0, 30.0, 29.9, 29.9, 29.8, 29.8, 29.6, 26.4, 23.0, 14.3; HRMS (FAB) Calcd for C$_{36}$H$_{71}$NNaO$_{10}$$^+$: 700.4970; Found: 700.4920.

4.1.25. (2S,3S,4R)-1-O-(α-D-Galactosyl)-6-oxa-2-tetracosanoylamino-1,3,4-octadecanetriol (11q)

^{1}H NMR (400 MHz, Pyr-d_5) δ = 8.47 (d, J = 8.7 Hz, 1H), 6.86 (br s, 1H), 6.62–6.42 (m, 3H), 6.36 (d, J = 6.3 Hz, 1H), 6.28 (br s, 1H), 5.54 (d, J = 3.8 Hz, 1H), 5.31–5.22 (m, 1H), 4.71–4.60 (m, 2H), 4.58–4.33 (m, 8H), 4.17 (dd, J = 2.6, 9.9 Hz, 1H), 4.04 (dd, J = 6.1, 9.9 Hz, 1H), 3.62–3.49 (m, 2H), 2.43 (dt, J = 1.6, 7.5 Hz, 2H), 1.80 (quin, J = 7.6 Hz, 2H), 1.64–1.55 (m, 2H), 1.40–1.16 (m, 58H), 0.90–0.85 (m, 6H); ^{13}C NMR (101 MHz, Pyr-d_5) δ = 173.4, 101.6, 74.3, 74.1, 73.1, 72.1, 71.9, 71.7, 71.0, 70.4, 68.7, 62.7, 51.6, 36.8, 32.2, 30.3, 30.1, 30.0, 29.9, 29.9, 29.8, 29.8, 29.6, 26.6, 26.4, 23.0, 14.3; HRMS (FAB) Calcd for C$_{47}$H$_{93}$NNaO$_{10}$$^+$: 854.6692; Found: 854.6697.

4.1.26. (2S,3S,4R)-1-O-(α-D-Galactosyl)-5-phenoxy-2-tetracosanoylamino-1,3,4-pentanetriol (11r)

^{1}H NMR (400 MHz, Pyr-d_5) δ = 8.56 (d, J = 8.7 Hz, 1H), 7.29–7.23 (m, 2H), 7.09–7.03 (m, 2H), 6.96–6.91 (m, 1H), 6.70 (br s, 1H), 5.56 (d, J = 3.8 Hz, 1H), 5.37–5.30 (m, 1H), 4.77–4.58 (m, 5H), 4.58–4.49 (m, 3H), 4.47–4.35 (m, 4H), 2.44 (dt, J = 2.1, 7.5 Hz, 2H), 1.80 (quin, J = 7.6 Hz, 2H), 1.38–1.17 (m, 40H), 0.87 (t, J = 6.9 Hz, 3H); ^{13}C NMR (101 MHz, Pyr-d_5) δ = 173.5, 160.1, 129.8, 120.8, 115.2, 101.6, 73.7, 73.1, 71.7, 71.6, 71.4, 71.0, 70.3, 68.6, 62.7, 51.5, 36.8, 32.1, 30.0, 30.0, 29.9, 29.9, 29.8, 29.8, 29.6, 26.4, 23.0, 14.3; HRMS (FAB) Calcd for C$_{41}$H$_{73}$NNaO$_{10}$$^+$: 762.5127; Found: 762.5139.

4.1.27. (3R,4S,5R)-4,5-O-Isopropylidene-1-(2,3,4,6-tetra-O-benzyl-α-D-galactosyl)-1-decyne-3,4,5-triol (14)

To a solution of **12** (92.7 mg, 0.17 mmol) in THF (2 ml) was added dropwise a solution of 1.57 M *n*-BuLi in hexane (120 μl, 0.19 mmol) at −45 °C, and the reaction temperature was raised to 0 °C. After 30 min of stirring the mixture was cooled to −48 °C and a solution of **13** (117 mg, 0.584 mmol) in THF (1.5 ml) was added. After 90 min of stirring the mixture was allowed to gradually warm to −30 °C. The mixture was quenched with 0.1 M phosphonate buffer (2 ml, pH 7.4) at −30 °C and allowed to warm to rt. Satd NaCl aq (5 ml) and water (40 ml) was added, and the product was extracted with EtOAc (40 ml × 1, 30 ml × 2). Combined organic layer was dried over Na$_2$SO$_4$, concentrated and purified by silica gel column chromatography (hexane/EtOAc; 9–25%) to yield **14** as a pale yellow oil (43.7 mg, 35% (47% based on recovered starting material)), along with its epimer (27.9 mg, 22% (30% br sm)) and recovered **12** (24.5 mg, 26%). ^{1}H NMR (400 MHz, CDCl$_3$) δ = 7.38–7.21 (m, 20H), 4.91 (d, J = 11.4 Hz, 1H), 4.86 (dd, J = 1.6, 5.7 Hz, 1H), 4.81 (d, J = 11.8 Hz, 1H), 4.74 (d, J = 11.8 Hz, 1H), 4.73 (d, J = 11.8 Hz, 1H), 4.67 (d, J = 11.8 Hz, 1H), 4.55 (d, J = 11.4 Hz, 1H), 4.48 (d, J = 12.2 Hz, 1H), 4.40 (d, J = 11.8 Hz, 1H), 4.38–4.33 (m, 1H), 4.15–4.04 (m, 4H), 3.96 (d, J = 1.6 Hz, 1H), 3.82 (dd, J = 2.8, 10.1 Hz, 1H), 3.55–3.49 (m, 2H), 2.65 (d, J = 3.7 Hz, 1H), 1.47 (s, 3H), 1.69–1.41 (m, 3H), 1.37 (s, 3H), 1.30–1.19 (m, 5H), 0.82 (t, J = 6.9 Hz, 3H); MS (FAB) 749 (M+H)$^+$.

4.1.28. (3R,4R,5R)-4,5-O-Isopropylidene-3-O-methanesulfonyl-1-(2,3,4,6-tetra-O-benzyl-α-D-galactosyl)-3,4,5-decanetriol (15)

To a warmed solution of **14** (15.6 mg, 0.021 mmol) and *p*-toluenesulfonylhydrazine (38.8 mg, 0.208 mmol) in dimethoxyethane was added 1 N NaOAc aq solution in 10 portions over 5 h. The mixture was stirred at 85 °C for 4.5 h after the final addition. After cooling to rt, the reaction was diluted with water (10 ml) and extracted with CH$_2$Cl$_2$ (30 ml × 1, 20 ml × 1, 10 ml × 1). Combined organic layers was dried over Na$_2$SO$_4$, concentrated and purified by silica gel column chromatography (hexane/EtOAc; 25%) to yield saturated alcohol as a colorless oil (14.2 mg, 91%). The alcohol was

dissolved in CH_2Cl_2 (1 ml) and pyridine (0.5 ml), and to the solution was added methanesulfonyl chloride (four drops) at 0 °C. After overnight stirring at rt the reaction was diluted with EtOAc (30 ml) and washed with satd NH_4Cl aq (20 ml) and water (10 ml). The organic layer was dried over Na_2SO_4, concentrated and purified over silica gel column chromatography (hexane/EtOAc; 25%) to yield compound **15** as a colorless oil (14.7 mg, 94%). ^{1}H NMR (400 MHz, $CDCl_3$) δ = 7.35–7.22 (m, 20H), 4.78–4.70 (m, 2H), 4.68 (s, 2H), 4.60 (s, 2H), 4.55 (d, J = 11.8 Hz, 1H), 4.49 (d, J = 11.4 Hz, 1H), 4.43 (d, J = 11.8 Hz, 1H), 4.11–4.04 (m, 2H), 3.99–3.92 (m, 2H), 3.88 (br s, 2H), 3.77–3.70 (m, 2H), 3.56 (dd, J = 4.7, 10.3 Hz, 1H), 3.08 (s, 3H), 1.97–1.46 (m, 5H), 1.44 (s, 3H), 1.33 (s, 3H), 1.32–1.22 (m, 7H), 0.88 (t, J = 6.9 Hz, 3H); MS (FAB) 831 (M+H)$^+$.

4.1.29. (3S,4S,5R)-4,5-O-Isopropylidene-1-(2,3,4,6-tetra-O-benzyl-α-D-galactosyl)-3-tetracosanoylamino-4,5-decanediol (16)

To a solution of **15** (14.7 mg, 0.0177 mmol) in DMF (1 ml) was added NaN_3 (18.0 mg, 0.277 mmol) at 0 °C, and the mixture was stirred at 90 °C for 17 h. After cooling to rt the mixture was diluted with EtOAc (50 ml), washed with water (30 ml × 3), dried over Na_2SO_4, concentrated and passed through silica gel column to give the crude azide. The crude azide was stirred overnight with Lindlar catalyst (14.6 mg) in EtOH (2 ml) under H_2 atmosphere. Insolubles were removed by passing through membrane filter, and the filtrate was concentrated to give amine as a pale yellow oil. A mixture of this amine, Lignoceric acid (11.7 mg, 0.0317 mmol), 1-hydroxy-7-azabenzotriazole (5.8 mg, 0.0426 mmol), Et$_3$N (3 drops), and 1-ethyl-3-(3-dimethylaminopropyl) carbodiimide hydrochloride (9.0 mg, 0.0469 mmol) in DMF (1 ml) and CH_2Cl_2 (1 ml) was stirred overnight at rt. The reaction was diluted with EtOAc (40 ml) and washed with satd $NaHCO_3$ aq (30 ml) and water (30 ml). The organic layer was dried over Na_2SO_4, concentrated and purified by silica gel column chromatography (hexane/EtOAc; 17% to 20%) to yield **16** as a colorless solid (9.3 mg, 48%). ^{1}H NMR (400 MHz, $CDCl_3$) δ = 7.35–7.22 (m, 20H), 5.68 (d, J = 8.9 Hz, 1H), 4.74 (d, J = 11.4 Hz, 1H), 4.68 (d, J = 12.2 Hz, 1H), 4.64 (d, J = 11.8 Hz, 1H), 4.63 (d, J = 11.8 Hz, 1H), 4.57–4.48 (m, 3H), 4.45 (d, J = 11.8 Hz, 1H), 4.06–3.99 (m, 2H), 3.99–3.92 (m, 4H), 3.87–3.74 (m, 2H), 3.68 (dd, J = 2.4, 7.7 Hz, 1H), 3.54 (dd, J = 4.3, 10.3 Hz, 1H), 2.10–1.99 (m, 2H), 1.40 (s, 3H), 1.30 (s, 3H), 1.83–1.13 (m, 54H), 0.88 (t, J = 6.5 Hz, 3H), 0.86 (t, J = 6.5 Hz, 3H); MS (FAB) 1103 (M+H)$^+$.

4.1.30. (3S,4S,5R)-1-(α-D-Galactopyranosyl)-3-tetracosanoylamino-4,5-decanediol (4)

A mixture of **16** in 80% AcOH was stirred at 60 °C for 3 h, after which all of the volatiles were removed and the residue was purified by silica gel column chromatography (hexane/EtOAc; 33% to 50%) to yield diol as a colorless solid (7.9 mg, 88%). A mixture of this diol and Pearlman's catalyst (10.6 mg) in MeOH (2.5 ml) and CH_2Cl_2 (1 ml) was stirred under H_2 atmosphere for 4.5 h. Insolubles were removed by passing through membrane filter, and washed thoroughly with mixed solution of MeOH and CH_2Cl_2. The filtrate was concentrated to give compound **4** as a colorless solid (5.4 mg, quant.). ^{1}H NMR (400 MHz, Pyr-d_5) δ = 8.41 (d, J = 9.0 Hz, 1H), 6.81–5.71 (m, 6H), 5.17–5.07 (m, 1H), 4.72 (dd, J = 5.5, 8.9 Hz, 1H), 4.57–4.45 (m, 3H), 4.36 (dd, J = 4.6, 11.2 Hz, 1H), 4.29–4.11 (m, 4H), 2.78–2.65 (m, 1H), 2.65–2.53 (m, 1H), 2.53–2.38 (m, 2H), 2.38–2.13 (m, 3H), 1.97–1.76 (m, 4H), 1.74–1.57 (m, 1H), 1.49–1.09 (m, 44H), 0.87 (t, J = 6.8 Hz, 3H), 0.81 (t, J = 7.2 Hz, 3H); ^{13}C NMR (101 MHz, Pyr-d_5) δ = 173.4, 78.5, 77.0, 73.8, 72.7, 72.2, 70.6, 70.4, 62.8, 52.7, 37.0, 34.5, 32.5, 32.1, 30.1, 30.0, 29.9, 29.9, 29.8, 29.6, 26.6, 26.2, 23.1, 23.0, 14.3; HRMS (FAB) Calcd for $C_{40}H_{79}NNaO_8{}^+$: 724.5698; Found: 724.5693.

4.2. Biological evaluation

4.2.1. In vitro cytokine production

Splenocytes were prepared from the spleens of C57BL/6 mice (6–8 weeks old, female) and suspended in a RPMI1640 medium (purchased from Nacalai) containing 10% fetal bovine serum (purchased from GIBCO), 5×10^{-5} M 2-mercaptoethanol (purchased from GIBCO), 1 mM pyruvate (purchased from SIGMA), and 25 mM HEPES (purchased from SIGMA). The cells (5×10^5 cells/well) were stimulated with glycolipid derivatives at a concentration of 100 ng/ml for 72 h at 37 °C in a 96-well flat bottom plate (purchased from IWAKI), and the concentration of IL-4 and IFN-γ in the culture supernatant were measured by ELISA (BD Pharmingen EIA Kit). Compound **2** was always included in the assay as a control and the cytokine release were expressed as relative to that of **2** for the mean of at least three experiments.

4.2.2. In vivo cytokine production

Each glycolipid was dissolved in 0.5% DMSO in saline. To clarify the antagonist activity of **4**, the compound was injected intravenously into C57BL/6 mice (9 weeks old, female) though tail vein at 0.1 μg/mouse, 15 min before OCH injection (0.1 μg/mouse). 3, 6, 9 h after second injection, sera were collected, and the content of serum IL-4 and IFN-γ were measured by ELISA (BioLegend ELISA Set). The data were presented as mean ± SD (N = 4–5). Statistical analysis was performed by Student's t-test by using JMP9.0.2 (SAS Institute Inc., Cary, NC).

4.2.3. In silico optimization of 2/hCD1d complex

Both acyl and phytosphingosine chain of **1** bound to hCD1d in the crystal structure was truncated in silico to correspond to **2**, and the complex thus obtained was further optimized. Optimization of the complex was performed stepwise as follows, utilizing Macromodel Ver. 9.0^{26} [force field OPLS2005/solv. Water] (convergence threshold .05 kJ/mol/Å): (i) main chain, Asp80, Asp151, Thr154 and ligand fixed, (ii) main chain, Asp80(Oδ1, Oδ2), Asp151(Oδ1, Oδ2), Thr154(Oγ) and oxygen atoms of the ligand fixed, (iii) main chain, distances among selected ligand atoms and Asp80, Asp151, Thr154 fixed, (iv) main chain fixed, (v) optimization of all the atoms.

Acknowledgements

References and notes

1. For recent reviews: (a) Joyce, S.; Girardi, E.; Zajonc, D. M. *J. Immunol.* **2011**, *187*, 1081; (b) Venkataswamya, M. M.; Porcelli, S. A. *Semin. Immunol.* **2010**, *22*, 68; (c) Van Kaer, L. *Immunol. Res.* **2004**, *30*, 139; (d) Wu, L.; Gabriel, C. L.; Parekh, W.; Van Kaer, L. *Tissue Antigens* **2009**, *73*, 535; (e) Cohen, N. R.; Garg, S.; Brenner, M. B. *Adv. Immunol.* **2009**, *102*, 1.
2. (a) Wu, D.; Xing, G.-W.; Poles, M. A.; Horowitz, A.; Kinjo, Y.; Sullivan, B.; Bodmer-Narkevitch, V.; Plettenburg, O.; Kronenberg, M.; Tsuji, M.; Ho, D. D. *Proc. Natl. Acad. Sci. U.S.A.* **2005**, *102*, 1351; (b) Zajonc, D. M.; Kronenberg, M. *Immunol. Rev.* **2009**, *230*, 188.
3. Zhou, D.; Mattner, J.; Cantu, C., III; Schrantz, N.; Yin, N.; Gao, Y.; Sagiv, Y.; Hudspeth, K.; Wu, Y.-P.; Yamashita, T.; Teneberg, S.; Wang, D.; Proia, R. L.; Levery, S. B.; Savage, P. B.; Teyton, L.; Bendelac, A. *Science* **2004**, *306*, 1786.
4. Wu, D.; Fujio, M.; Wong, C.-H. *Bioorg. Med. Chem.* **2008**, *16*, 1073.
5. (a) Morita, M.; Motoki, K.; Akimoto, K.; Natori, T.; Sakai, T.; Sawa, E.; Yamaji, K.; Koezuka, Y.; Kobayashi, E.; Fukushima, H. *J. Med. Chem.* **1995**, *38*, 2176; (b) Morita, M.; Sawa, E.; Yamaji, K.; Sakai, T.; Natori, T.; Koezuka, Y.; Fukushima, H.; Akimoto, K. *Biosci., Biotechnol., Biochem.* **1996**, *60*, 288; (c) Takikawa, H.; Muto, S.; Mori, K. *Tetrahedron* **1998**, *54*, 3141; (d) Graziani, A.; Passacantilli, P.; Piancatelli, G.; Tani, S. *Tetrahedron: Asymmetry* **2000**, *11*, 3921.
6. Yu, K. O. A.; Porcelli, S. A. *Immunol. Lett.* **2005**, *100*, 42. and references cited therein.

7. Liang, P.-H.; Imamura, M.; Li, X.; Wu, D.; Fujio, M.; Guy, R. T.; Wu, B.-C.; Tsuji, M.; Wong, C.-H. *J. Am. Chem. Soc.* **2008**, *130*, 12348.
8. (a) Yang, G.; Schmieg, J.; Tsuji, M.; Franck, R. W. *Angew. Chem., Int. Ed.* **2004**, *43*, 3818; (b) Schmieg, J.; Yang, G.; Franck, R. W.; Tsuji, M. *J. Exp. Med.* **2003**, *198*, 1631.
9. (a) Miyamoto, K.; Miyake, S.; Yamamura, T. *Nature* **2001**, *413*, 531; (b) Yamamura, T.; Miyake, S. PCT Int. Appl. WO 2003/016326, 2003; *Chem. Abstr.* **2003**, *138*, 205292m.; (c) Yamamura, T.; Miyamoto, K.; Illes, Z.; Pal, E.; Araki, M.; Miyake, S. *Curr. Top. Med. Chem.* **2004**, *4*, 561; (d) Oki, S.; Chiba, A.; Yamamura, T.; Miyake, S. *J. Clin. Invest.* **2004**, *113*, 1631.
10. Chiba, A.; Oki, S.; Miyamoto, K.; Hashimoto, H.; Yamamura, T.; Miyake, S. *Arthritis Rheum.* **2004**, *50*, 305.
11. Borg, N. A.; Wun, K. S.; Kjer-Nielsen, L.; Wilce, M. C. J.; Pellicci, D. G.; Koh, R.; Besra, G. S.; Bharadwaj, M.; Godfrey, D. I.; McCluskey, J.; Rossjohn, J. *Nature* **2007**, *448*, 44.
12. Koch, M.; Stronge, V. S.; Shepherd, D.; Gadola, S. D.; Mathew, B.; Ritter, G.; Fersht, A. R.; Besra, G. S.; Schmidt, R. R.; Jones, E. Y.; Cerundolo, V. *Nat. Immunol.* **2005**, *6*, 819.
13. Henon, E.; Dauchez, M.; Haudrechy, A.; Banchet, A. *Tetrahedron* **2008**, *64*, 9480.
14. McCarthy, C.; Shepherd, D.; Fleire, S.; Stronge, V. S.; Koch, M.; Illarinov, P. A.; Bossi, G.; Salio, M.; Denkberg, G.; Reddington, F.; Tarlton, A.; Reddy, B. G.; van der Merwe, P. A.; Bersa, G. S.; Jones, W. Y.; Bartisa, F. D.; Cerundolo, V. *J. Exp. Med.* **2007**, *204*, 1131.
15. Murata, K.; Toba, T.; Nakanishi, K.; Takahashi, B.; Yamamura, T.; Miyake, S.; Annoura, H. *J. Org. Chem.* **2005**, *70*, 2398.
16. Toba, T.; Murata, K.; Nakanishi, K.; Takahashi, B.; Takemoto, N.; Akabane, M.; Nakatsuka, T.; Imajo, S.; Yamamura, T.; Miyake, S.; Annoura, H. *Bioorg. Med. Chem. Lett.* **2007**, *17*, 2781.
17. Schmidt, R. R.; Maier, T. *Carbohydr. Res.* **1988**, *174*, 169.
18. The anomeric diastereomers were separable by column chromatography over silica gel. The stereochemistry of the galactoside linkage was determined by ^{1}H NMR spectra. The anomeric proton of the α-isomer appears more downfield than β-isomer (typically $\sim$0.5 ppm) and shows smaller coupling constant (typically less than 5 Hz). Example data of the anomeric proton (400 MHz, CDCl$_3$): For the α-isomer **9** (R = *n*-Bu): δ 4.94 (d, *J* = 3.5 Hz, 1H), and its corresponding β-isomer: δ 4.41 (d, *J* = 7.7 Hz, 1H).
19. Taniguchi, M.; Kawano, T.; Koezuka, Y. PCT Int. Appl. WO1998/044928A, 1998, 129, 310889.
20. Toba, T.; Murata, K.; Yamamura, T.; Miyake, S.; Annoura, H. *Tetrahedron Lett.* **2005**, *46*, 5043.
21. Dondoni, A.; Mariotti, G.; Marra, A. *J. Org. Chem.* **2002**, *67*, 4475.
22. Ohtani, I.; Kusumi, T.; Kashman, Y.; Kakisawa, H. *J. Am. Chem. Soc.* **1991**, *113*, 4092–4096.
23. Annoura, H.; Murata, K.; Yamamura, T. PCT Int. Appl. WO2004/072091, 2004; *Chem. Abstr.* **2004**, *141*, 225769n.
24. Michieletti, M.; Bracci, A.; Compostella, F.; De Libero, G.; Mori, L.; Fallarini, S.; Lombardi, G.; Pnaza, L. *J. Org. Chem.* **2008**, *73*, 9192.
25. MAESTRO Ver. 7.5.112; Schrödinger, LLC: New York.
26. Macromodel Ver. 9.0 (Schrödinger, LLC): Mohamadi, F.; Richards, N. G. J.; Guida, W. C.; Liskcamp, R.; Lipton, M.; Caufield, C.; Chang, G.; Hendrickson, T.; Still, W. C. *J. Comput. Chem.* **1990**, *11*, 440.

CASE REPORT

Clinical improvement in a patient with neuromyelitis optica following therapy with the anti-IL-6 receptor monoclonal antibody tocilizumab

Manabu Araki · Toshimasa Aranami ·
Takako Matsuoka · Masakazu Nakamura ·
Sachiko Miyake · Takashi Yamamura

Abstract Neuromyelitis optica (NMO) is a disabling autoimmune disease associated with an elevation of anti-aquaporin 4 (AQP4) autoantibodies. Here, we present a case with NMO who responded to monthly administration of the anti-IL-6 receptor antibody tocilizumab. The treatment rapidly reduced the elevated numbers of plasmablasts and anti-AQP4 autoantibodies in the patient. Furthermore, neuropathic pain and disability scores gradually improved. Tocilizumab may be considered as a therapeutic option for NMO.

Keywords Interleukin-6 · Neuromyelitis optica · Plasmablast · Tocilizumab

Introduction

Neuromyelitis optica (NMO) is an inflammatory disease of the central nervous system (CNS) characterized by recurrent episodes of destructive inflammation that target mainly the optic nerves and spinal cord. Patients with NMO often suffer from persistent neurological complications, including blindness, neuropathic pain, or difficulty walking. Previously, the identity of NMO was controversial because

of its resemblance to multiple sclerosis (MS), but there is now international consensus that NMO is a distinct disease associated with elevated pathogenic autoantibodies specific for aquaporin 4 (AQP4) water channel protein [1, 2]. Whereas multiple sclerosis (MS) is classified as a CNS demyelinating disease, the hallmarks of NMO pathology are a loss of AQP4 in astrocytes, perivascular deposits of immunoglobulins with complements, and severe necrosis with macrophage and granulocyte infiltration [3]. There is an increasing amount of evidence to support the notion that anti-AQP4 antibodies are involved in the immune-mediated injury to astrocytes which occurs in NMO. In fact, in vivo injection of anti-AQP4 antibody causes the complement-dependent destruction of astrocytes [4] and enhances the manifestations of rodent experimental autoimmune encephalomyelitis (EAE) [5].

Acute exacerbations of NMO usually respond to intravenous methylprednisolone (IVMP). However, plasmapheresis may be given to cases with NMO who are refractory to IVMP. This is a reasonable therapy for NMO, considering the pathogenic role of anti-AQP4 antibodies [6]. In contrast, the effects of disease-modifying drugs prescribed for MS, including interferon β (IFNβ) [6, 7], natalizumab [8], and fingolimod [9], are unpredictable and could even exacerbate the disease activity of NMO. Therefore, oral corticosteroid and an immunosuppressant such as azathioprine (AZA) are broadly used to prevent relapses of NMO. More recently, B-cell-depleting anti-CD20 antibody, rituximab, has shown some therapeutic efficacy in NMO [10]. An interpretation by the authors is that targeting anti-AQP4 antibody-producing cells might be an attractive therapeutic option for NMO.

We recently reported that plasmablasts (PB), a subpopulation of B cells, are the main producers of anti-AQP4 antibody, and that PB are increased in number in the

M. Araki · T. Yamamura (✉)
Multiple Sclerosis Center, National Center Hospital,
National Center of Neurology and Psychiatry,
4-1-1 Ogawa-Higashi, Kodaira, Tokyo 187-8551, Japan
e-mail: yamamura@ncnp.go.jp

T. Aranami · T. Matsuoka · M. Nakamura · S. Miyake ·
T. Yamamura
Department of Immunology, National Institute of Neuroscience,
National Center of Neurology and Psychiatry,
4-1-1 Ogawa-Higashi, Kodaira, Tokyo 187-8502, Japan

🌋 Springer

peripheral blood of patients with NMO [11]. We also found that exogenous IL-6 promotes the production of anti-AQP4 antibody from PB in vitro, whereas serum IL-6 level is elevated in active NMO in vivo [11]. Overall, these results suggest that IL-6 receptor (IL-6R) signaling pathways are involved in the pathogenesis of NMO.

IL-6, originally identified as a differentiation-inducing factor of B cells [12], is now known to play a variety of roles in autoimmunity and chronic inflammation. In fact, the anti-IL-6 receptor antibody tocilizumab (TCZ), humanized anti-IL6R monoclonal antibody, proved to be efficacious in rheumatoid arthritis (RA), juvenile idiopathic arthritis, and Castleman disease (CD) [13]. Of note, anti-IL-6R antibody may inhibit the survival of anti-AQP4 antibody-producing PB in vitro [11]. Therefore, we set up a clinical study to explore the efficacy of TCZ in vivo in the treatment of NMO ["The safety and efficacy of tocilizumab in patients with neuromyelitis optica" (SET-NMO); UMIN000005889]. Here, we describe alterations in immunological parameters and clinical manifestations in the first registered patient with NMO [14].

Case report

A 36-year-old female patient first complained of back pain and numbness on her trunk and lower extremities in May 1998. Because of T2-weighted MRI scans showing a high-intensity lesion on the thoracic spine (Th10-11) and an episode of clinical relapse, she was tentatively diagnosed with MS, and IFNβ-1b treatment was started in combination with low-dose oral prednisolone (PSL) in May 2002. After measurement of anti-AQP4 antibody confirmed the diagnosis of NMO, IFNβ was stopped and switched to a
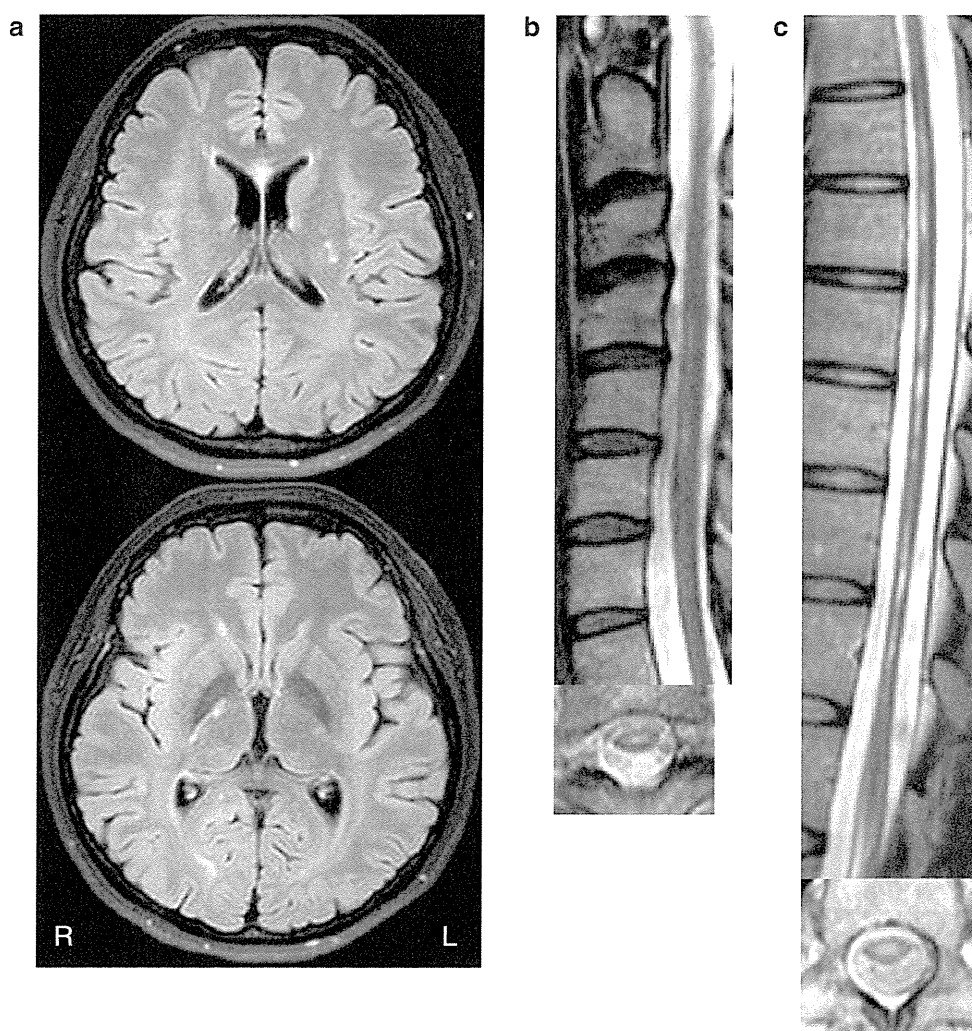

Fig. 1 MRI before TCZ administration. **a** MRI showed multiple high-intensity lesions in the corpus callosum, left putamen, and right posterior limb of the internal capsule on T2-weighted images. **b, c** T2-weighted cervical and thoracic MRI demonstrates extensive scattered high-intensity lesions involving central gray matter

combination of PSL and AZA in January 2008. However, she had six relapses in 2010 and two relapses in the first half of 2011. She consented to participate in the SET-NMO study and was admitted in October 2011 for first administration of TCZ.

On admission, she had left ptosis, hypoesthesia in distal limbs, truncal and plantar paresthesia, and hyperreflexia in all extremities. The Expanded Disability Status Scale of Kurtzke (EDSS) [15] was 3.5. Her gait was spastic and she complained of pain on walking, with a score of 4 judged on the numeric rating scale (NRS) [16]. A blood test was unremarkable except for increased levels of total cholesterol [275 mg/dl; reference range 128–219], LDL cholesterol [159 mg/dl; 70–139], and triglyceride [262 mg/dl; 30–149]. Serum IL-6 was normal 1.6 pg/dl (reference < 4.1), and antinuclear antibody, anti-SS-A and SS-B antibodies were negative. A cerebrospinal fluid (CSF) test was also unremarkable [IgG index 0.46, negative oligoclonal IgG bands, and IL-6 1.6 pg/dl]. No gadolinium-enhanced lesion was detected on brain MRI (Fig. 1a). T2-weighted spinal cord MRI showed high-intensity lesions consistent with longitudinally extensive transverse myelitis (LETM), a hallmark of NMO (Fig. 1b, c). Central conduction times of sensory evoked potentials on upper and lower extremities were within the normal limits. Visual evoked potential and auditory brainstem response were also normal.

Intravenous TCZ of 8 mg/kg was given monthly to the patient for six months until April 2012. As clinical outcome measures, we evaluated the number of relapses and changes in EDSS and NRS. Serum levels of IL-6, PB, and anti-AQP4 antibody were also examined. The PB frequency (CD19$^+$CD27^{high}CD38^{high}CD180$^-$ cells) was measured by flow cytometry (FACS Canto II, BD Biosciences), as described previously [11]. Serum anti-AQP4 antibody titers were estimated by measuring the binding of IgG in the serum to AQP4 transfectants, as previously described (with minor modifications) [11]. Median fluorescence intensity (MFI) values were obtained from indirect FITC-anti-human antibody staining. The MFI values were measured for serially diluted serum from the patient. The cut-off value for the MFI was determined by calculating the average of the values for six healthy subjects + 3 × SEM.

Four days after the first administration of TCZ, she developed a minor relapse with truncal paresthesia and gait disturbance. However, she experienced no relapse afterwards and the sensory disturbances and pain in her extremities and trunk gradually improved. The NRS score decreased from four to zero within four administrations (Fig. 2a). She could walk for more than 1 h without any assistance and her EDSS improved to 2.0 (Fig. 2a).

Oral PSL was tapered from 13 mg to 6 mg daily during the six courses of TCZ. AZA was also reduced in six months from 50 mg every second day to 50 mg weekly (Fig. 2b). The serum IL-6 level immediately increased after the TCZ treatment, and the high IL-6 value persisted until the second administration of TCZ (Fig. 3a). In contrast, the frequency of PB as well as the anti-AQP4 antibody titer reduced within the first month (Fig. 3a, b). The frequency of PB increased to 34 % at six months (before the sixth administration). We assume that this increase in

Fig. 2 Clinical course after TCZ administration. a Follow-up for EDSS and NRS. b Dosages of concomitant drugs given to the patient (AZA and PSL). Numbers from 1–6 show the timing of each TCZ administration. URI upper respiratory infection